FAST NEUTRON ACTIVATION DOSIMETRY WITH TLDS

by

David W. Pearson and P. R. Moran

Medical Physics Laboratories

Departments of Physics and Radiology

University of Wisconsin

Madison, Wisconsin 53706

USERDA Technical Report COO-1105-227

CONTRACT NO. E(11-1)-1105

DISCLAIMER

Abstract

FAST NEUTRON ACTIVATION DOSIMETRY WITH TLDS

By

David W. Pearson

Under the supervision of Professor P. R. Moran

Fast neutron activation using threshold reactions is the only neutron dosimetry method which offers complete discrimination against gamma-rays and preserves some information about the neutron energy. Conventional activation foil technique requires sensitive radiation detectors to count the decay of the neutron induced activity. For extensive measurements at low neutron fluences , vast outlays of counting equipment are required. TL dosimeters are inexpensive, extremely sensitive radiation detectors. The work of Mayhugh et.al. (Proc. Third Int. Conf. on Luminescence Dosimetry, Risø Report 249 , 1040, (1971)) showed that $CaSO_4$:Dy TLDs could be used to measure the integrated dose from the decay of the radioactivity produced in the dosimeters by exposure to thermal neutrons. This neatly combines the activation detector and counter functions in one solid state device. This work has been expanded to fast neutron exposures and other TL phosphors. The reactions $^{19}F(n,2n)^{18}F$, $^{32}S(n,p)^{32}P$, $^{24}Mg(n,p)^{24}$, and $^{64}Zn(n,p)^{64}Cu$ were found useful for fast neutron activation in commercial TLDs. As each TLD is its own integrating decay particle counter, many activation measurements can be made at the same time. The subsequent readings of the TL signals can be done serially after the induced radioactivity has decayed, using only one TL reader. The neutron detection sensitivity is limited mainly by the number statistics of the neutron activations. The precision of the neutron measurement is within a factor of two of conventional foil activation for comparable mass detectors. Commercially available TLDs can measure neutron fluences of $10^9 n/cm^2$ with 10% precision.

P R Moran
Prof. Physics and Radiology

ACKNOWLEDGEMENTS

I thank Professor P. R. Moran for his support and encouragement and Professor J. R. Cameron for his patience, guidance and help in editing this manuscript.

I thank Dr. Jerome Wagner for his interest and valuable aid during the initial part of this study, and Dr. M. R. Mayhugh for discussions and suggestions. Mr. Jerome Lasky rendered valuable help with the apparatus.

Special thanks are due to Richard Cashwell and the crew at the UW Nuclear Reactor, Steve, Larry and Gerry for their friendly and generous assistance with some of the neutron exposures.

Thanks are also due to colleagues Drs. Luis Barroilhet and Phil Cohen for many discussions and general encouragement.

I thank Ms. Alice Rocca for typing the manuscript and Orlando Canto for his valuable aid in preparing the figures.

This work was supported by the U. S. Energy Research and Development Administration under contract E (11-1) 1105.

TABLE OF CONTENTS

LIST OF FIGURES

LIST OF TABLES

CHAPTER I

INTRODUCTION

Fast neutrons, those with energies in the range from 10 keV to 20 MeV, are of increasing interest and importance to radiobiologists, medical and health physicists. Both radionuclide and accelerator sources of fast neutrons are readily available. Effective use of fast neutrons in biology and medicine requires the development of convenient and accurate dosimetry techniques.

The responses of biological systems to ionizing radiation depend on the absorbed energy or dose (the unit of dose is the rad, 1 rad= 100 ergs/gm) and on the microscopic spatial distribution of the dose expressed as the LET (Linear Energy Transfer usuall given in keV/μ).[1] The exact bioresponse dependencies are different for different biological syatems and for different radiation effects.[2,3] Fast neutrons deliver dose to biological materials through recoil protons and larger nuclear fragments. These secondary particles are very densely ionizing, having mean LETs in excess of 10keV/μ.[3] Because of their small interaction cross sections, fast neutrons penetrate biological materials readily and are the only practical means for exposing objects tens of centimeters thick to uniform, high LET radiation.[2]

High LET radiation is generally more effective at killing cells than low LET radiation.[2] This is particularly true for the anoxic cells in tumors.[4] The recognition of the greater Relative Biological Effectiveness (RBE) of fast neutrons stimulated interest in fast neutron therapy.[5]

There are many approaches to radiation dosimetry depending on the prior knowledge one has and the information one seeks. The ideal dosimeter would be a device with a readily measured physical property whose response to a radiation field is isomorphic to the particular response exhibited by the system of interest in that same field. The dosimeter must also offer some advantage over simply observing the system of interest, such as being cheaper, easier to measure, faster in response or perhaps non-living.

With respect to biological systems, the response is usually parameterized in terms of the dose and its spatial distribution or LET. For gamma- and x-rays the secondary particles are electrons; the LET is small and the effective atomic number, Z, of the medium is the most important consideration in determining the dose and the bio-response. For gamma- and x-ray dosimeters, "tissue equivalent" means only having the same average or effective Z as tissue. Since fast neutrons interact only with nuclei, "tissue equivalent" for neutrons requires the dosimeter to have the same atomic composition as tissue.[6] This requirement correctly provides the primary ionizations and secondary particle distributions, but does not account for events like bond breakage, radical formation and scavenging, polymerization or biological repair. These and other de-excitation effects make the neutron induced bioresponses deviate from proportionality to dose alone. Either the neutron energy distribution or the distribution in LET of the dose is also required for an adequate description.

A further complication to measuring neutron dose is that neutron beams are usually accompanied by gamma-rays. It is not sufficient to

measure the total, i.e., neutron dose plus gamma dose, as the neutrons have a much larger relative biological effectiveness per unit dose which depends on the neutron energy.

A tissue equivalent proportional counter which counts recoil proton pulses can be biased to minimize its gamma-ray sensitivity.[7] The LET and dose can be calculated from a pulse height spectrum for neutron energies greater than about 3 MeV. For lower neutron energies, the recoil proton pulses are difficult to separate from gamma-ray pulses. It is also possible with pulse shape discrimination to use organic scintillators as neutron dosimeters.[8] Both dose and energy information can be obtained if corrections for the nonlinearity of the light output with neutron energy and for wall and end effects are made. While these devices are very sensitive, they require active electronics and are not particularly small.

Another approach to neutron dosimetry is to measure the neutron fluence and energy spectrum in order to calculate the tissue dose. A common method of measuring neutron fluence, which has the advantage of being insensitive to gammas, is activation dosimetry. For fast neutrons, endothermic reactions, which require a minimum or threshold neutron energy to produce a radioactive product are most useful. The measured activity of the radioactive product, A_d, is related to the incident neutron fluence by

$$A_d = F(t, t_c, t_{\frac{1}{2}}) N_p \int_0^{E_{max}} \sigma(E)\, \Phi(E)\, dE \,. \qquad 1$$

In Eq. 1, F gives the dependence of the activity on the time of measurement t, the exposure time t_e and the half life of the product $t_{1/2}$; N_p is the number of the parent nuclei which is assumed to be a constant; $\sigma(E)$ is the nuclear cross section as a function of energy for the reaction; and $\Phi(E)$ is the neutron fluence as a function of energy E. The value of the integral is the only information about the neutron energy distribution preserved by the reaction. For any one particular threshold reaction all that can be concluded is that some neutrons with energies greater than the threshold were present. To determine the neutron energy spectrum, several different threshold reactions are used and a set of simultaneous equations of the form of Eq. 1 must be solved for $\Phi(E)$. A more complete discussion of this problem and appropriate solution techniques using expansions in orthogonal functions is given by Routti.[9]

In addition to their complete gamma-ray discrimination, activation dosimeters can be small and have moderate sensitivity. Their main disadvantages are that most of the cross sections are not accurately known, an integral dose response obtains only for short exposures and measuring the induced radioactivity requires sensitive counters with active electronics. Extensive activation measurements require vast arrays of counters, particularly for small fluences when the resulting low induced activity requires long counting times, precluding the serial counting of several dosimeters on one counter. It would be of considerable value then to find some inexpensive and convenient method of measuring low level neutron induced radioactivity.

Solid state dosimeters based on the phenomenon of thermoluminescence (TL), are inexpensive, passive, integrating and can be made extremely small while retaining high sensitivity. TL dosimeters have been used to measure low level natural radioactivity and released activity distribution patterns.[10] TL dosimetry is discussed extensively in textbooks and the proceedings of several conferences.[11] Only a brief digression through a simplified model is presented here.

Virtually any transparent, insulating solid of adequate purity can be made to exhibit thermoluminescence. The essential requirement is for defects to be present in the solid, some of which function as localized traps for the electrons and holes and some as recombination centers which convert the recombination energy of these electrons and holes into light. Some fraction of the electrons and holes generated by ionizing radiation are immobilized by the trapping centers. Subsequent thermally activated release of these trapped charges, by heating the material, results in their recombination. The fraction of these recombinations which occurs at the appropriate, optically active recombination centers produces light. The trapped charges must be sufficiently stable to avoid spontaneous loss at ambient temperature, yet releasable at temperatures low enough that incandescence is small.

The trapping and luminescence centers in commercial TL phosphors are associated with impurities intentionally added during preparation. The trapping centers and luminescence centers are usually associated with different kinds of impurities. Most luminescent centers involve the transition elements and the rare earths. The emission spectrum

of the TL is characteristically determined by these elements. The nature of the trapping centers is less well known. The impurity levels which give the maximum TL signal are of the order of 10^{-4}, (0.01 - 0.1 mole %). These concentrations are small but the impurities cannot be completely ignored when calculating the radiation response of a dosimeter.

A simplified energy diagram model of the TL process is shown in Fig. 1. This model assumes the electron to be the mobile charge. Models with mobile holes and tunneling processes have been considered.[12,13] To the extent that the fraction of electrons trapped and the fraction of recombinations giving rise to luminescence are independent of previous ionizations, the TL emitted will be proportional to the absorbed dose. Deviations from a linear response can be expected when the density of ionizations along a track exceeds the trap density (as occurs with high LET radiation), and when the number of tracks becomes large enough to give overlap between traps and recombination centers belonging to different tracks (as obtains at moderately high dose[14]).

In general, TL phosphors show a much lower response to fast neutrons than to equal doses of beta- or gamma-rays. The high LET recoil nuclei from fast neutron reactions do not efficiently produce TL because of enhanced prompt recombination and saturation of the traps near the recoil track. This is similar to the reduced efficiency exhibited by scintillators for high LET radiation.[15] TL phosphors are also non-hydrogenous so that the neutron generated dose to the dosimeter is less than the dose to tissue for the same fluence.

Figure 1. TL Model Energy Diagram

A) The situation in a completely annealed material. There are no electrons or holes in the shallow traps.

B) The electron-hole pair produced by ionizing radiation, in this case taken to be an x-ray, are trapped separately in some set of traps.

C) Due to thermal lattice vibrations, indicated by $\hbar\omega$, during heating the electron is remobilized. Eventually some small fraction of these remobilized electrons will encounter the luminescent recombination center and release some of its excess energy as a TL photon, $h\nu$.

D) The luminescent center is then returned to its original state by the diffusion of a thermally mobilized hole from a nearby hole trap or perhaps by a tunneling process of the electron to a nearby hole.

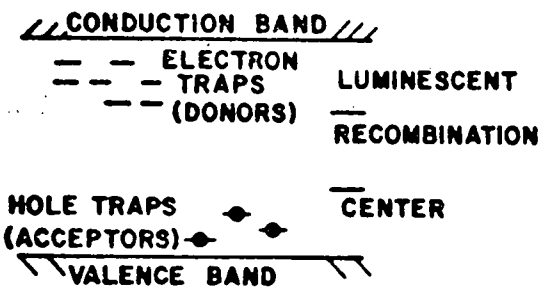
CONDUCTION BAND
ELECTRON
TRAPS
(DONORS)
LUMINESCENT
RECOMBINATION
CENTER
HOLE TRAPS
(ACCEPTORS)
VALENCE BAND

A

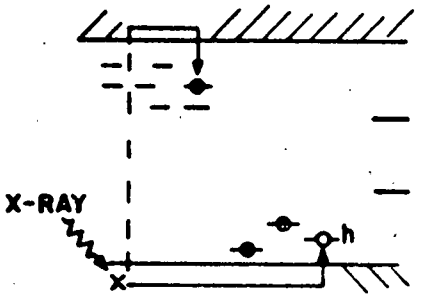
X-RAY
h
x

B

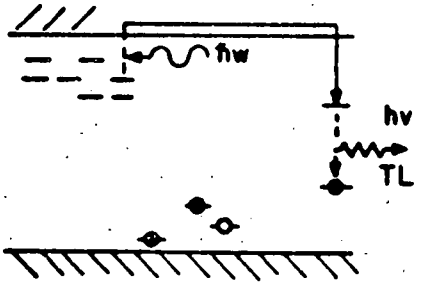
hw
hv
TL

C

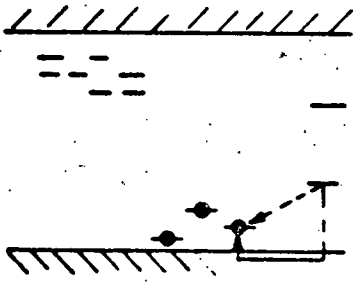

D

The fast neutron response of TL dosimeters can be increased by embedding the phosphor grains in a hydrogenous matrix. An additional TL signal due to the recoil protons is observed. However, due to the lower efficiency of TL production for high LET particles, the total TL signal is not proportional to the neutron plus gamma dose. The proton dose must be calculated from the difference in response between dosimeters in hydrogenous and non-hydrogenous matrices. At present no good method of obtaining the neutron energy or the secondary particle LET spectrum has been demonstrated.

The LiF Thermoluminescent Dosimeters (TLDs) have a thermal neutron sensitivity dependent on the abundance of the ^{6}Li isotope. The reaction is $^{6}Li(n,\gamma)^{3}H$ with a cross section of 950 barns which decreases proportional to $1/E_n$ at higher neutron energies E_n. Thermal neutron fluences can be measured from the difference between ^{6}Li containing dosimeters (natural abundance 7% or enriched 95% ^{6}Li) and ^{7}LiF dosimeters (99.99% ^{7}Li). Fast neutrons can detect by moderating them to thermal energies. Moderating assemblies which give adequate response to fast neutrons are large, 30 to 50 cm in diameter.

For personnel monitoring, a large, mobile moderating structure is readily available, namely the body itself. Thermal neutron detectors of the ^{6}Li - ^{7}LiF type have been developed to measure the albedo of thermal neutrons produced by the body in a fast neutron fluence.[16,17] Cadmium shields are used over the side of the detector assembly away from the body to reduce the response to thermal neutrons from the external environment. The response of these albedo dosimeters depends on the incident fast neutron energy. While valuable

for radiation protection purposes in known neutron environments, this energy dependence limits the accuracy of albedo dosimeters in situations where the neutron energy spectrum is not known.

In short, TL dosimeters are excellent for beta- and gamma-ray dosimetry, but have features which limit their direct application to fast neutron dosimetry. These features are the generally lower TL response neutrons than to gamma-rays, the dependence of the TL response on neutron energy being greater for thermal neutrons than for fast neutrons and the lack of information on the incident neutron energy spectrum. Used in conjunction with activation techniques however, the excellent beta-ray response of TL dosimeters can be applied to fast neutron dosimetry. Kocher and Endres reported using TL to measure the neutron activation of rhodium foils.[18] Mayhugh and co-workers reported using a TL phosphor to measure the dose delivered by the decay of its own thermal neutron induced radioactivity.[19] Mayhugh's technique, briefly, was to expose the TL phosphor to a neutron fluence, producing radioactivity as with ordinary activation foils. The TL produced by this exposure, "prompt dose" is thermally removed and the dosimeters left in a cool dark place while the neutron induced activity decays. The subsequently measured TL signal, "delayed dose" is proportional to the dose from the decay of that activity. This neatly combines the activation detector and counter functions in one small, inexpensive, solid state device. Since each dosimeter is its own counter, there is virtually no limit to the number of activation measurements which can be made

in the same fluence. This thesis investigates the applicability of this TL activation technique to fast neutron dosimetry.

The next chapter discusses the important characteristics of the TL dosimeter phosphors. The neutron activations available in the dosimeters studied are listed. The procedure developed for the delayed dose method of activation dosimetry is described in Chapter III. The apparatus used for the delayed dose measurements and the radiation sources used are described in Chapter IV. The measurement of these delayed dose response of the TL dosimeters to thermal and 14 MeV neutrons is described in Chapter V. Chapter VI discusses the use of the delayed dose method to measure the attenuation of a 14 MeV neutron beam and to characterize a fission neutron fluence. The discussion of the measurement results and an assessment of the possible applications of the delayed dose method are given in Chapter VII.

REFERENCES

1. ICRU (1962) defines LET to be the quotient of dE_c/dl where dE_c is the average energy locally imparted to the medium by a charged particle traversing the distance dl. ICRU Report 10e available as NBS Handbook 88 from the Superintendent of Documents, U. S. Government Printing Office, Washington, D. C. 20402.

2. J. J. Broerse, Effects of Energy Dissipation by Monoenergetic Neutrons in Mannalian Cells & Tissues. Radiobiological Institute TNO of the Organization for Health Research, TNO, Rijswijle, Netherlands, (1966).

3. W. K. Sinclair, "Radiobiological Dosimetry," Chpt. 29 in Radiation Dosimetry, Vol. III, Attix & Roesch, eds., Academic Press, New York, (1969).

4. G. W. Barendsen, H. M. D. Walter, J. F. Fowler and D. K. Bewley, Radiat. Res. 18, 106, (1963).
   D. K. Bewley, European J. of Cancer 7, 99, (1971).

5. J. F. Fowler, R. L. Morgan, C. A. P. Wood, D. K. Bewley, R. H. Thomlinson, S. Hornsey, G. Silini, T. Alper, B. A. Turner and J. A. Silverstein, Brit. J. Radiology 36, 77, (1963).

6. Specification of the composition of the standard man is given in NBS Handbook 75, Superintendent of Documents, U. S. Government Printing Office, Washington, D. C. 20402.

7. G. S. Hurst, Brit. J. Radiology 27, 353, (1954).
   E. B. Wagner and G. S. Hurst, Rev. Sci. Instr. 29, 1953, (1958).

8. R. Batchelor, W. B. Getboy, J. B. Parker and J. H. Towle, Nucl. Instr. and Methods 13, 70, (1961).

9. J. T. Routti, UCRL Report 18514, U. of Cal. Rad. Lab., Berkeley, CA, (1969).

10. For example the natural radioactivity of pottery sherds. V. Mejdahl, Proc. 2nd Int. Conf. on Luminescence Dosimetry, P. 868; S. J. Fleming, ibid., P. 464; M. J. Aitken, ibid., P. 281. Available as CONF 680920 from the Clearinghouse for Federal Scientific and Technical Information, National Bureau of Standards, U. S. Department of Commerce, Springfield, VA 22151; also "Released Activity Distributions of ^{85}Kr," B-I. Ruden, Report AE 362, Aktiebolaget Atomenergi, Stockholm, Sweden, (1969).

11. TL textbooks include:

Thermoluminescence Dosimetry, J. R. Cameron, N. Suntharalingam and G. Kenney, U. W. Press, Madison, WI 53706, (1968).

Solid State Dosimetry, Klaus Becker, Chemical Rubber Press, Cleveland, OH.

Radiation Dosimetry, Vol. II, F. H. Attix, W. C. Roesch and E. Tochlin, eds., Chpt. 13 "Solid State Integrating Dosimeters," J. F. Fowler and F. H. Attix.

The proceedings of four international conferences on luminescence dosimetry are valuable references.

The first, held at Stanford, California in June, 1965, is available as CONF 650657 from Clearinghouse for Federal Scientific and Technical Information, Springfield, VA 22151.

The second, held at Gatlinburg, Tennessee in Sept., 1968, is available as CONF 680920 from the same address.

The third, held in Risø, Denmark in Oct., 1971, is available as a three volume set. Risø Report No. 249 from Jul. Gjellerup, 87, Solvgade, DK-1307, Copenhagen, Denmark.

The fourth, held in Krakow, Poland, in Aug., 1974, is available in three volumes as the Proceedings of the Fourth International Conference on Luminescence Dosimetry from the Institute of Nuclear Physics Library, Krakow, Poland.

12. E. W. Claffy, "TL and Color Centers in LiF," P. 74, CONF 650637, Clearinghouse for Federal Scientific and Technical Information, Springfield, VA 22151.

C. C. Klick, E. W. Claffy, S. G. Gorbics, F. H. Attix, J. H. Schulman and J. G. Allard, J. Appl. Phys. 38, 3867, (1967).

13. M. R. Mayhugh, N. M. Johnson and R. W. Christy, J. Appl. Phy. 41, 2968, (1970).

M. R. Mayhugh and R. W. Christy, J. Appl. Phy. 41, 4775, (1970).

14. F. H. Attix, Proc. 4th Int. Conf. on Luminescence Dosimetry, P. 31, Institute of Nuclear Physics Library, Krakow, Poland, (1974)

15. J. B. Birks, The Theory and Practice of Scintillation Counting, Macmillan, New York, (1964).

16. J. B. C. Brown, F. M. Gayton, J. A. Hall, J. R. Harvey and G. A. M. Webb, "Recommendations Concerning the Use of the Personal Neutron Albedo Dosimeter," Repnt. RD/B/R328, Berkeley, Nuclear Laboratories, June, 1967, Central Electricity Generating Board, U. K.

17. J. E. Hoy, Health Phys. 23, 385, (1972).

18. L. F. Kocher and G. W. R. Endres, P. 552, CONF 680920, Clearinghouse for Federal Scientific and Technical Information, Springfield, VA 22151.

19. M. R. Mayhugh, S. Watanabe and R. Mucillo, Risø Reports 249, P. 1040, Jul. Gjellerup, 87, Solvgade, DK-1307, Copenhagen, Denmark, (1971).

CHAPTER II

DOSIMETER PHOSPHOR MATERIALS

To do neutron activation dosimetry with TL dosimeters, it is important to appreciate the following properties of the phosphors: (1) the neutron reactions which produce significant delayed dose TL, (2) the dosimetric sensitivity and stability of the TL, and (3) the dosimeter forms which are available. This chapter discusses these properties for the LiF:Ti,Mg, CaF_2:Dy, Mg_2SiO_4:Tb, ZnO:Tm, and $CaSO_4$:Dy phosphors. The significant neutron reactions in these phosphors are summarized in Table I.

Lithium Fluoride: The most widely used TL phosphor is LiF:Mg,Ti, probably because of its nearly tissue equivalent response to x-rays. The principal fast neutron activation of LiF is $^{19}F(n,2n)^{18}F$. The threshold energy for this reaction is about 11 MeV. However, the cross section becomes appreciable only for neutron energies greater than about 12 MeV. The ^{18}F nucleus decays by positron emission 97% of the time. The remaining 3% of the decays go by electron capture. The maximum positron energy is 0.64 MeV, giving a maximum range of about 0.4 mm. The half life is 110 min. The fluorine concentration is 2.3×10^{22} atoms/gm, which gives about 5.3×10^{20} atoms per 23 mg dosimeter. All other reactions with appreciable cross section give nuclides with half lives either too short to be observed, e.g., ^{16}N, $t_{1/2}$=7.2 sec, or ^{19}O, $t_{1/2}$=29 sec, or too long to have a measurable activity, e.g., ^{3}H, $t_{1/2}$=12.3 yr. Thus LiF:Mg,Ti activation measures only fast neutrons, with energies greater than 12 MeV.

TABLE I

List of TL Phosphors and Available Neutron Reactions

Phosphor	Reaction	Threshold	Cross Section	Decay Mode	Half Life
LiF:Mg,Ti (TLD-700)	$^{19}F(n,2n)^{18}F$	12 MeV	50mb @ 14 MeV	β^+, .64 MeV	109 min
CaF_2:Dy (TLD-200)	$^{19}F(n,2n)^{18}F$	12 MeV	50mb @ 14 MeV	β^+, .64 MeV	109 min
	$^{164}Dy(n,\gamma)^{165}Dy$	Thermal	2.8 kb	β^-, 1.3 MeV	140 min
CaF_2:Mn	$^{19}F(n,2n)^{18}F$	12 MeV	50mb @ 14 MeV	β^+, .64 MeV	109 min
	$^{55}Mn(n,\gamma)^{56}Mn$	Thermal	13 b	β^-, 2.8 MeV	2.5 hr
$CaSO_4$:Dy	$^{32}S(n,p)^{32}P$	2.5 MeV	250mb @ 14 MeV	β^-, 1.7 MeV	14 day
	$^{164}Dy(n,\gamma)^{165}Dy$	Thermal	2.8 kb	β^-, 1.3 MeV	140 min
ZnO:Tm	$^{64}Zn(n,p)^{64}Cu$	4 MeV	200mb @ 14 MeV	EC, β^+, .6 MeV	12.8 hr
	$^{68}Zn(n,\gamma)^{69}Zn$	Thermal	1 b	β^-, .9 MeV	57 min
Mg_2SiO_4:Tb	$^{24}Mg(n,p)^{24}Na$	7 MeV	200mb @ 14 MeV	β^-, 2.8 MeV	15 hr

The glow curve of LiF shown in Figure 2 consists of five principal peaks between room temperature and 250°C. The magnesium impurity is considered to be associated with this trap distribution. Peaks numbered (4) and (5) are the main dosimetry peaks. Their thermal behavior is complex.[1] Peaks (1) and (2) decay by first order kinetics with room temperature half lives of 10 min. and 10 hr. respectively. Peak (3), which is poorly resolved, has an apparent first order decay half life of a few months. During the decay of peaks (2) and (3), some of the traps responsible for these peaks convert into the traps responsible for peaks (4) and (5).[2] In samples which have been annealed to remove the lower temperature peaks, peaks (4) and (5) show first order decay half lives of 7 years and 80 years respectively at room temperature.

Because of the conversion of the lower temperature peaks (11% of peak (2) and 60% of peak (3)) into the main dosimetry peaks, neither the peak height nor the integrated light sum of peaks (4) and (5) is independent of time between exposure and readout for samples which have not been specially annealed. This effect is not a simple electronic retrapping of thermally released charge, as it is independent of whether the traps are filled or not.[3] A special pre-irradiation annealing at 80°C for one day removes most of the first three peaks until the dosimeter is heated again.[4] Rather than use this somewhat inconvenient annealing procedure, the integration temperatures have been adjusted as shown in Fig. 2 to give a light sum which is constant within a few per cent for at least two days. The standard deviation of the measurement of successive 100 mR exposures is about 3%.

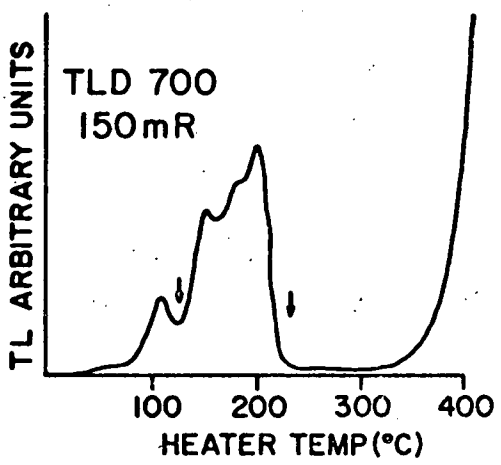

Figure 2. Glow Curve of Lithium Fluoride (TLD-700).

The arrows show the limits of integration for the light sum. The TL scale in arbitrary units is essentially the same scale used for each glow curve in the chapter (Figs. 2-7).

LiF exhibits a linear TL response with dose up to about 10^3 rad. The supralinear response observed for greater doses reaches a maximum increased sensitivity of a factor of 6 at about 3×10^4 rads.[5] This increased sensitivity can be retained for subsequent exposures provided the dosimeter is not heated above 300°C.[6] At the large exposures required for this sensitization, several more TL peaks appear at temperatures greater than 250° C. If these higher temperature traps are not emptied, thermally activated and uv induced processes cause the repopulation of the main dosimetry peaks.[7] The tails of these peaks also have appreciable intensity at the temperatures of peaks (4) and (5). To exploit the phenomenon of sensitization for low dose measurements, the combined uv bleaching and thermal annealing technique of Mayhugh and Fullerton is required.[8] This procedure eliminates the thermal and optical transfer and reduces the residual tails of the higher temperature TL peaks which would otherwise limit the minimum measurable dose to a few tenths of a rad. The sensitized phosphor shows no supralinearity.

The TL emission spectrum of LiF:Mg,Ti is a broad, composite band with its peak at a wavelength of about 400nm associated with the titanium impurity.[9] The sensitized phosphor has the same emission spectrum.[10] The S-11 photocathode response is a good match to the TL emission of LiF:Mg,Ti.

Most measurements with TL dosimeters have been of gamma- or x-ray fields. The TL response to betas is the same on a rad basis provided the betas penetrate the bulk of the dosimeter.[11] The assumption that beta emitters internal to the phosphor produce a TL response

which is linear with dose for small doses and which is proportional to the x-ray sensitivity is reasonable. This assumption allows the relative TL responses of different dosimeters to be determined by exposure to a calibrated gamma-ray source.

The irreversible sensitivity increases observed by Mason[12] and by Alexander[13] after exposure of LiF to neutrons was not observed for any of the LiF dosimeters used in this study.

TLD grade LiF:Mg,Ti is available from several sources as powder, powder embedded in teflon sheets or rods, extruded rods or ribbons and single crystals. The most useful form for low level readiation measurements is the extruded ribbon, about 3.2 x 3.2 x 0.9 mm^3 containing about 23 mg of phosphor.* This form is the most convenient to handle and exhibits the least spurious signal. Both natural abundance (7.5% ^6Li) and 7 LiF (99.99% ^7Li) are available.

Calcium Fluoride: Calcium fluoride is a host material for several TL phosphors. CaF_2:Mn, CaF_2:Dy and CaF_2:(natural) are the best known. Calcium fluoride doped with manganese was developed at the US Naval Research Laboratory.[14,15]

The principal fast neutron reaction is $^{19}F(n,2n)^{18}F$. CaF_2 has 1.5×10^{22} fluorine atoms per gram, about two thirds that of LiF. The intrinsic TL sensitivity of CaF_2:Mn is about ten times that of LiF (depending on Photodetector response) so that the overall neutron response per gram is greater.

---

* Available from Harshaw Chemical Company, Solon, Ohio.

The manganese in CaF_2:Mn is the luminescent activator at a concentration of 3 mole %. The ^{55}Mn isotope has a large thermal neutron cross section of 13 barns for the reaction $^{55}Mn(n,\gamma)^{56}Mn$. There are also several resonances listed for this reaction in the energy range from 1 - 10^3eV. The resonance integral $\int\sigma(E)(1/E)dE$ = 14 barns.[16] The number of manganese activations per gram of CaF_2 for low energy neutrons is thus about three times the number of fluorine activations for a similar fluence of fast neutrons. The 2.5 hour half life of ^{56}Mn is close enough to the 110 minute half life of ^{18}F to prevent separation of their contributions to the TL.

A single broad glow peak appears at about 260°C as shown in Fig. 3. The background of incandescence from the heater and hot phosphor rises under the high temperature wing of the glow peak. This background makes the accurate and reproducible setting of the high temperature integration limit both difficult and essential. Discrimination against the incandescence with color filters is also difficult since the TL emission is at relatively long wavelengths, peaking at about 500 nm.

While one would expect a TL peak at 260°C to be stable at room temperature, an anamolous fading of the stored TL of 5% in the first day is observed.[15] Exposure to fluorescent room lights (65 fc) increases this fading to 5% in ten minutes. Annealing at 500°C for five minutes completely removes the TL. The response of CaF_2:Mn is linear with dose and shows no sensitization.[16] Readings of successive 100mR exposures to gamma-rays from ^{137}Cs show standard deviations

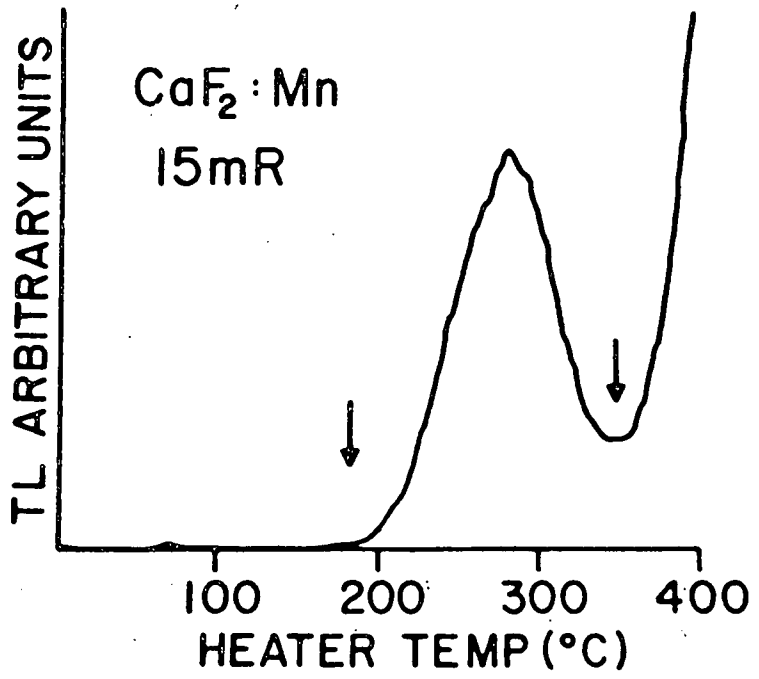

Figure 3. Glow Curve of Calcium Fluoride: Manganese.

The arrows show the integration limits for the light sum.

of about 1%. The sensitivities among the pressed chip CaF_2:Mn dosimeters used in this study ranged as much as a factor of two making individual calibration essential.*

Calcium fluoride doped with dysprosium is commercially available as TLD-200 in extruded or powder forms. The extruded ribbons are the preferred form.**

The principal fast neutron reaction is again $^{19}F(n,2n)^{18}F$. The dysprosium luminescent activator is present at a concentration of about 0.1 mole %. However, the enormous cross section of 2.8 kilobarns for the thermal neutron reaction $^{164}Dy(n,\gamma)^{165}Dy$ compensates for the low concentration. The half life of ^{165}Dy, $t_{1/2}$=140 mins is sufficiently close to that of ^{18}F, $t_{1/2}$=110 mins, to preclude separately measuring their activities from their contributions to the TL signal.

CaF_2:Dy was characterized by Binder and Cameron who found a complex, four peaked glow curve which showed some batch dependence and changed as a function of exposure.(17) The glow curve of the CaF_2:Dy dosimeters used in this study is shown in Fig. 4. The integrated TL signal between the limits shown fades approximately 12% in one day at room temperature. Most of this decrease is in the low temperature peaks, but as these are poorly resolved, it is difficult to set the integration limits to exclude them. Exposure to room lights (65 fc) increases the fading rate threefold with the decrease being more uniformly distributed over all the peaks.

---

* The dosimeters used in this study are no longer available, but the CaF_2:Mn phosphor is available from the Harshaw Chemical Company, Solon, Ohio.

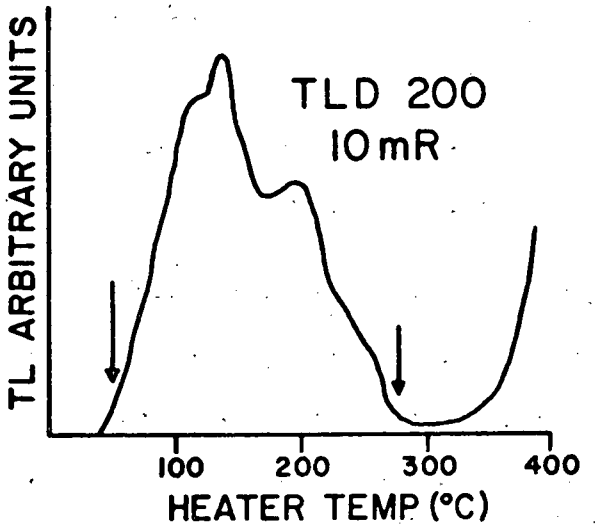

Figure 4. Glow Curve of Calcium Fluoride: Dysprosium (TLD-200). The arrows show the integration limits for the TL light sum.

For exposures less than 600 R, the TL response is linear with exposure. No sensitization is observed. The reproducibility of a single dosimeter is about 4% for successive exposures of 100mR: Most of this variation is believed to be due to the instability of the low temperature peaks.

The emission spectrum of CaF_2:Dy is characteristic of the Dy^{+3} ion. There are two main emission peaks at 483.5 nm and 576.5 nm with a smaller peak at 460 nm. The TL sensitivity thus depends on the wave length response of the Photomultiplier Tube (PMT) and measured values vary from ten to thirty times that of LiF.

Magnesium Silicate: Magnesium silicate doped with terbium, Mg_2SiO_4:Tb, was developed in Japan as a high sensitivity phosphor with a more tissue equivalent response for x-rays than the other high sensitivity phosphors such as CaF_2 and $CaSO_4$.[18] The principal fast neutron reaction is $^{24}Mg(n,p)^{24}Na$. This reaction has a threshold energy of about 6 MeV. The ^{24}Na nuclide decays with a half life of 15 hours by the emission of a beta-ray with a maximum energy of 2.8 MeV. The range of such a beta-ray is about 0.3 mm in Mg_2SiO_4:Tb. There are about 6.7×10^{21} atoms of ^{24}Mg per gram of phosphor.

While the Mg_2SiO_4:Tb phosphor has no interfering reactions, the sodium in the glass capillary encapsulation activates with thermal neutrons. The thermal reaction is $^{23}Na(n,\gamma)^{24}Na$, with a cross section of half a barn. The amount of sodium in the glass is unknown. Since the same radionuclide is produced, fast neutron and thermal neutron activations cannot be distinguished.

The glow curve of Mg_2SiO_4:Tb exhibits a single peak at about 190°C (Fig. 5). The TL output after exposure initially increases with time, reaching its maximum value in less than one hour.[19] The fading from this maximum is less than 3% in two months at 30°C. However, exposure of the irradiated phosphor to room light can reduce the TL by a factor of two within ten minutes.[19] This optical bleaching shows complex kinetics which depend on the magnitude of the gamma-ray exposure and intensity of the uv portion of the room lights. Room light will induce a TL signal in an unirradiated dosimeter equivalent to a 10 mR gamma-ray exposure in ten minutes.

The TL emission of Mg_2SiO_4:Tb appears white to the eye and consists of many bands between 380 nm and 600 nm.[18] The TL sensitivity depends on the PMT response and values between 30 and 100 times that of LiF have been observed.

The individual capillary dosimeters measure successive 10 mR exposures to gamma-rays with a standard deviation of 5%. Because of their cylindrical symmetry, the dosimeters cannot be oriented reproducibly. Much of the 5% variation is believed to be from different orientations on successive measurements. The variation in sensitivity among different dosimeters is as great as 15%.

Beside the glass capillary dosimeters, this phosphor is available embedded in a silicone resin. The embedded forms are unsuited for low dose measurements as a non-radiation induced TL signal equivalent to 100 mR is present.*

---

* From Dai Nippon Toryu Company, 1060 Naruta, Odawara, 250, Japan.

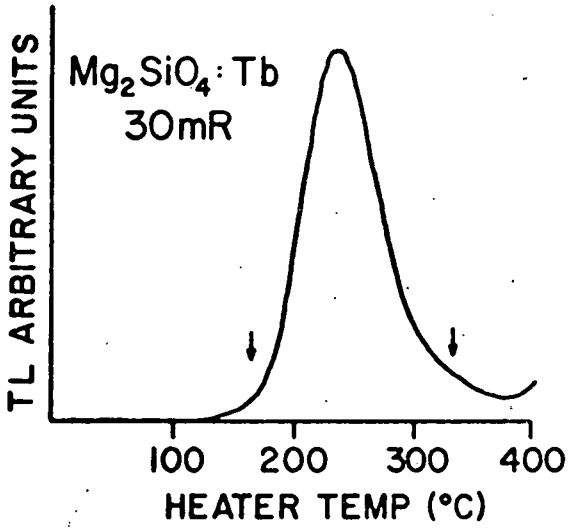

Figure 5. Glow Curve of Magnesium Silicate: Terbium.

The arrows indicate the integration limits for the light sum.

Zinc Oxide: Zinc oxide doped with thulium, ZnO:Tm, is an extremely sensitive phosphor which has not been fully characterized. The material used in this study is in the form of an ungraded powder of hexagonal crystals ranging from 1mm long prisms to less than 0.01mm thick platelets. A commercial source for this phosphor has not been identified.

The principal fast neutron reaction in ZnO:Tm is $^{64}Zn(n,p)^{64}Cu$. The copper decays with a half life of 12.8 hours by electron capture, beta or positron emission. The maximum beta energy is 0.6 MeV. The principal interfering reactions are $^{64}Zn(n,2n)^{63}Zn$, for fast neutrons with a cross section of 200 mb at a neutron energy of 14.6 MeV. The half life of ^{63}Zn is 38 mins, decaying by positron emission with a maximum energy of 2.3 MeV. For thermal neutrons, the reaction $^{68}Zn(n,\gamma)^{69}Zn$ has a cross section of 1 barn. The half life of ^{69}Zn is 57 mins against decay by beta emission with a maximum energy of 0.6 MeV. The relative abundances of these stable Zinc isotopes are: ^{64}Zn=49%, ^{68}Zn=18.5%.

The TL glow curve of ZnO:Tm has a main peak at about 220°C with smaller peaks at 120°C add 60°C as seen in Fig. 6. The peak at 60°C fades in a few minutes. The peak at 120°C fades with a room temperature half life of about three days. The main peak fades less than 3% in one month. Exposure to fluorescent room lights (65 fc) increases the fading to about 3% in ten minutes. Unirradiated phosphor acquires about 0.1 mR equivalent TL from a ten minute room light exposure.

The TL response of ZnO:Tm is linear with exposure up to at least 10R. Larger exposures have not been investigated. Annealing at 500°C

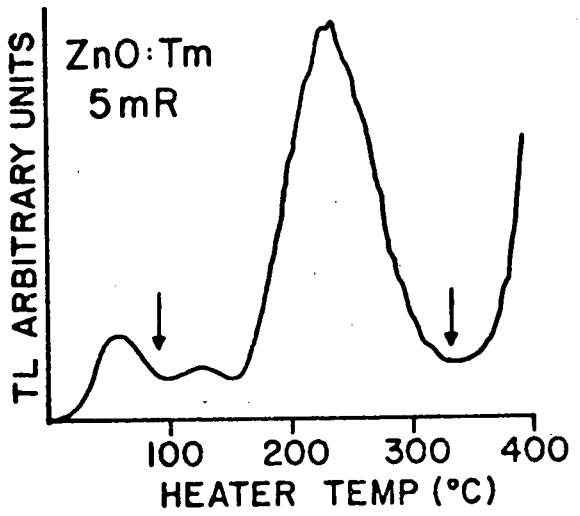

Figure 6. Glow Curve of Zinc Oxide: Thulium.

The arrows indicate the limits of integration for the light sum.

for five minutes in air empties the TL traps and resets the sensitivity. Successive exposures to 10 mR of gamma-rays can be measured with a standard deviation of 2%. The major source of this variation is believed to be changes in the distribution of the powder in the silver pan between measurements. Since powder samples thicker than a monolayer of grains show self absorption of the TL, the maximum useful sample size is about 40 mg.

The TL emission spectrum of ZnO:Tm has not been measured but appears to the eye to be an intense blue.

Calcium Sulfate: Calcium sulfate is probably the oldest and most sensitive TL phosphor. $CaSO_4$:Mn was used by Hoffman in 1897 to investigate electrons and x-rays,[20] and by Lyman in 1935 to detect vacuum ultraviolet photons.[21] However, the manganese activator produces a relatively unstable TL trap, and fading at room temperature of 7% per hour is observed. Yamashita and co-workers produced calcium sulfate doped with dysprosium or thulium having the sensitivity of $CaSO_4$:Mn but with a stable trap and a more suitable emission.[22] $CaSO_4$:Dy is commonly available as powder and as powder embedded in teflon.*

The fast neutron reaction of interest in $CaSO_4$:Dy is $^{32}S(n,p)^{32}P$. The ^{32}P half life is 14 days, emitting a beta with maximum energy of 1.7 MeV. The range of such a beta is about 0.3 mm in $CaSO_4$. There are about 4.4×10^{21} atoms of sulfur per gram of $CaSO_4$.

---

* Harshaw Chemical Company, Solon, Ohio.

The dysprosium is activated by thermal neutrons via the $^{164}Dy(n,\gamma)^{165}Dy$ reaction which has a thermal neutron cross section of 2.8 kilobarns. The reaction has a cross section of the order of barns extending out to neutron energies greater than 1 MeV. The half lives of the ^{32}P ($t_{1/2}$=14 days) and ^{165}Dy ($t_{1/2}$=140 mins) are sufficiently different that their activities can be separately determined by measuring the delayed dose TL at two different times. The first measurement at one day includes almost all of the dysprosium decay and about 5% of the phosphorus decay. The activity of the phosphorus is then determined from a subsequent measurement after an additional 14 days.

The glow curve of $CaSO_4$:Dy consists of one principal peak at about 220°C and two small peaks at lower temperatures as seen in Fig. 7. The peak at 220°C fades less than 2% per month at room temperature. Exposure to room lights increases this fading threefold. Exposure of an unirradiated sample to sunlight produces a TL signal equivalent to about 10 mR in an hour.(23) Similar characteristics obtain for $CaSO_4$:Tm.(23)

Calcium sulfate responds linearly with exposure up to 10^3R. A small supralinearity appears for larger exposures although no sensitization occurs. Annealing for 5 mins at 500°C empties the TL traps and restores the original sensitivity. Successive exposures of a 25 mg powder sample to 10 mR of gamma-rays can be measured with a standard deviation of 3%. As with all loose powders, changes in the distribution of the phosphor between measurements contributes much of this variation. Exposures as small as 0.1 mR can be measured with 20

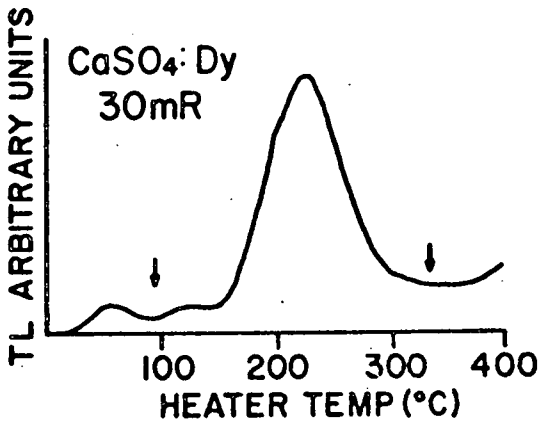

Figure 7. Glow Curve of Calcium Sulfate: Dysprosium.

The arrows indicate the integration limits for the light sum.

to 50% precision. However, a non-radiation induced TL signal is often encountered which is the equivalent of 0.1 mR.

The emission spectrum of $CaSO_4$:Dy consists of two main bands at 480 nm and 570 nm.[20] These bands are due to the $^4F_{9/2} \rightarrow {}^6H_{13/2}$ and $^4F_{9/2} \rightarrow {}^6H_{13/2}$ transitions respectively of the Dy^{+3} ion. This emission provides a reasonable match to the spectral sensitivity of the S-11 response PMT. $CaSO_4$:Dy is about 100 times as sensitive to x-rays as LiF.

REFERENCES

1. D. W. Zimmerman, C. R. Rhyner and J. R. Cameron, USAEC Report COO-1105-101 and Health Phys. 12, 325, (1966).
2. T. L. Johnson "Optimum Integrating Period for Unannealed LiF TLDs," note to be published in Health Physics.
3. L. F. Booth, T. L. Johnson and F. H. Attix, Health Phys. 23, 137, (1972).
4. R. Buch, unpublished data, University of Wisconsin, (1962). Quoted in Thermoluminescent Dosimetry, J. R. Cameron, N. Suntharalingan and G. N. Kenney, University of Wisconsin Press, Madison, WI, (1968).
5. D. W. Zimmerman, R. Bland and J. R. Cameron, USAEC Report, TID-19112, (1963).
6. C. R. Wilson, L. A. DeWerd and J. R. Cameron, USAEC Report, COO-1105-116, (1966).
7. D. W. Pearson and J. R. Cameron, USAEC Report, COO-1105-140, (1965) and COO-1105-149, (1969).
8. M. R. Mayhugh and G. D. Fullerton, Health Phys. 28, 297, (1975).
9. S. G. Gorbics, CONF 650637, P. 167. Available from the Clearinghouse for Federal Scientific and Technical Information, Springfield VA 22151.
10. D. W. Pearson and J. R. Cameron, USAEC Report, COO-1105-123, (1966)

    J. Thompson, D. Phil, Thesis, Oxford University, Oxford, U. K., (1970).

    L. A. DeWerd and T. Stoebe, Phys. Med. Biol. 17, 187, (1972).

11. J. Kastner, R. Hukkoo and B. G. Oltman, CONF 650637, P. 482.
B. C. Oltman, J. Kastner, P. Tedeschi and J. H. Beggs, Health Phys. 13, 918, (1967).
U. Greitz and B.-I. Ruden, Phys. Med. Biol. 17, 193, (1972).

12. E. W. Mason, Phys. Med. Biol. 15, 79, (1970).

13. A. Alexander, Dept. Nucl. Engr., Kansas State University, Manhattan, KS, private communication, June, 1973.

14. R. J. Ginther and R. D. Kirk, NRL Prog. Report, Sept., 1956; J. Electro Chem. Soc. 104, 365, (1957).

15. J. H. Schulman, Rev. Sci. Instr. 31, 1263, (1960); Nucleonics 18, 92, (1960).

16. M. Prokic, Proc. Third Int. Conf. on Luminescence Dosimetry, Risø Report #249, Part III, P. 1051, (1971). Jul. Gjellerup, 87, Solvgade, DK-1307, Copenhagen, Denmark.

17. W. Binder and J. R. Cameron, Health Phys. 17, 613, (1969).
A complete survey of the TL from CaF_2:Rare Earth Phosphors is given by J. L. Merz and P. S. Pershan, Phys. Rev. 162, 217 and 235, (1967).

18. T. Hashizume, Y. Kato, T. Nakajina, T. Toryu, H. Sakamoto, N. Kotera and S. Eguchi; Advances in Physical and Biological Radiation Detectors, IAEA-SM-143/11, P. 91, (1971), IAEA, P. O. Box 590, A-1011 Vienna, Austria.

19. H. Sakamoto, Phys. Med. Biol. 15, 139, (1970).

20. M. W. Hoffman, Ann. Phys. Chem. (NF) 60, 269, (1897).

21. T. Lyman, Phys. Rev. 48, 149, (1935).

22. T. Yamashita, N. Nada, H. Onishi and S. Kitamura, CONF 680970, P. 4, (1968), Clearinghouse for Federal Scientific and Technical Information, Springfield, VA 22151.

23. T. Nakajima, Health Phys. 23, 133, (1972).

24. R. L. Dixon and K. E. Ekstrand, Phys. Med. Biol. 19, 196, (1974).

CHAPTER III

DOSIMETRY PROCEDURES

This chapter describes a convenient procedure for using commercially available TL dosimeters for neutron activation dosimetry. Ideally, such a procedure should require a minimum of critically timed steps and complicated calibrations. The principal value of the delayed dose technique described here is its potential for the parallel processing of many dosimeters with a small amount of equipment. Convenience and simplicity will be considered as well as maximum sensitivity. The discussion will be in five parts: Activation, annealing, storage, readout, and analysis.

Activation: The exposure of TL phosphors to neutrons results in the production of radioactive nuclei of various types according to the standard differential equation:

$$\frac{d}{dt}N_A(t) = -\lambda_A N_A(t) + N_P \int_0^{E_{max}} \sigma_A(E)\, \phi(E,t)\, dE , \qquad 2$$

where $N_A(t)$ is the number of nuclei of radioisotope A at time t and λ_A is their decay constant ($= .69/t_{1/2}$); N_P is the number of original nuclei in the phosphor which can be activated to A. The differential cross section for the reaction is $\sigma_A(E)$, and $\phi(E,t)$ is the differential neutron flux.

The general solution of Eq. 2 has the form

$$N_A(t_e) = N_P \int_0^{t_e} \int_0^{E_{max}} \sigma_A(E)\, \phi(E,t)\, e^{-(t_e - t)\lambda_A}\, dE\, dt . \qquad 3$$

The zero of time has been chosen to coincide with the beginning of the exposure so that t_e is both the time at the end of the exposure and the length of the exposure. Two cases provide simple, closed form expressions for Eq. 3. The first is the short exposure case, defined by $t_e < (10\,\lambda_A)^{-1}$. If we assume $N_A(0) = 0$, then

$$N_A(t_e) = N_p \int_0^{E_{max}} \sigma(E)\, \Phi(E)\, dE\,, \qquad 4$$

where $\Phi(E)$, the differential neutron fluence, is given by

$$\Phi(E) = \int_0^{t_e} \phi(E,t)\, dt. \qquad 5$$

For short exposures, the induced activity is proportional to the neutron fluence. The only available information about the incident neutron energy is contained in the value of the integral.

The second is the constant flux case, that is $\phi(E,t) = \Phi(E)$. The solution is

$$N_A(t_e) = \frac{N_p}{\lambda_A}\left[1 - \exp(-\lambda_A t_e)\right] \int_0^{E_{max}} \sigma_A(E)\, \phi(E)\, dE\,. \qquad 6$$

As $t_e \to \infty$ the saturated activity or maximum N_A is approached. The subsequent decay of the radioactive nuclei follows the relation

$$N_A(t) = N_A(t_e) \exp -\lambda_A (t - t_e)\,. \qquad 7$$

From the condition of the short exposure case, one can set limits on the range of useful half lives. For the induced activity to be proportional to the neutron fluence, the half life of the activated nuclide needs to be long compared to the anticipated exposure time. The condition $t_{1/2} > 10t_e$ assures that the activation in the worst case is proportional to the fluence within 7%. For exposure times of about ten minutes, the minimum useful half life is then about two hours.

Shorter lived nuclides could be used to determine flux rates for the constant flux case. However, the short lived nuclides require rapid handling after exposure to avoid serious loss of activity before it can be measured. The presence of short lived nuclides in a phosphor having a useful activation is a potential source of error.

Since it is the decay of the activated nuclides which is measured, very long lived half lives are also of little value. The radiation from long lived nuclides is not sufficiently greater than background to be measured accurately. Preferred half lives are less than a day. The presence of long lived nuclides in a phosphor having a useful activation produces an apparently greater background radiation and reuse of the dosimeter must be considered carefully.

The above expressions assume that the neutron flux is uniform over the volume of the dosimeter. Since TL dosimeters are typically less than half a centimeter in diameter, uniformity holds for most neutron fields. The absorption of neutrons by the dosimeter itself might also perturb the flux. The product $\eta_p \sigma$, where η_p is the number of precursor nuclei per cm^3, is the reciprocal of the neutron absorption length. If $d << (\eta_p \sigma)^{-1}$ where d is the appropriate maximum linear dimension of

the dosimeter, this self absorption can be neglected. For fast neutron reactions the cross sections are all small enough that self shielding is not a problem. For thermal neutron reactions the cross sections are often very large, but as long as the concentrations of the activating nuclides are small no appreciable absorption occurs.

Further consideration of the product $\eta_p \sigma$ suggests that, since most fast neutron cross sections are generally smaller than one barn ($10^{-24} cm^2$), only nuclei which are principal constituents of the phosphor will be activated to any useful extent. As a corollary however, impurities which are present in small amounts but which have enormous cross sections for thermal neutrons (e.g., rare earth activator dysprosium) can produce appreciable activity. A list of the commercially available TL dosimeters and the neutron activations possible is given in Table I.

Annealing: In addition to inducing radioactivity, the exposure of TL dosimeters to fast neutrons produces a TL signal from both the direct fast neutron interactions and from the gamma-rays which are usually present in laboratory "neutron" beams. This prompt dose TL is two to three orders of magnitude greater than the delayed dose TL from the subsequent decay of the neutron induced activity. To measure the delayed dose, the prompt dose must be removed completely. A thermal annealing in air in a furnace at 510°C for five minutes suffices for all the phosphors discussed here.

During the time interval between the end of the exposure at time t_e and the cooling of the dosimeters to ambient after the annealing at time t_a, the activity has decayed to the fraction $\exp -\lambda_A(t_a - t_e)$ of

its initial value. Thus this time interval, $(t_a - t_e)$, should be made as small as possible and accounted for during data analysis. The maximum heating and cooling rates which are easily obtained and the minimum time required at the annealing temperature set the shortest possible annealing time interval.

For ease in handling, the solid dosimeters are placed in holes milled into thin aluminum blocks, numbered for identification. The blocks are covered with a layer of aluminum foil to keep out light. Up to twenty dosimeters can be annealed in one block at the same time. The blocks and dosimeters reach 500°C about 3 minutes after being placed in the 510°C furnace. After remaining two minutes longer, they are removed and cooled in contact with a lead block at room temperature. This cooling takes an additional two minutes. The cooling rate affects the TL sensitivity of the LiF dosimeters and must be reproduced reasonably well. The shortest time interval $(t_a - t_e)$ is 7 minutes.

Powder dosimeters which were exposed in gelatine or polyethylene capsules are transferred to aluminum foil packets and given the same annealing. Since all dosimeters considered here show some optical sensitivity, after annealing they should be handled under safe light conditions.

Storage: After cooling, the dosimeters in their holders are placed in an area of low background radiation while the neutron induced radioactivity decays. During this time, the TL signal grows according to the equation

$$TL(t_r) = K\left[\sum_A N_A(t_a) D_A f_A (1-\exp-\lambda_A t_{ra}) + d_B f_B t_{ra}\right] , \qquad 8$$

in which the time of readout is t_r and the storage interval is $t_{ra}=t_r-t_a$, with all times measured from the initiation of the exposure. The constant k describes the reader sensitivity in photons counted per TL photon emitted. This depends on the quantum efficiency of the phototube, the aperture of the optics, the presence of optical filters and the wavelength of the emitted light. The summation is over the A different unstable nuclides whose numbers at the end of annealing are $N_A(t_a)$. The average energy deposited from one decay of nucleus A is D_A and f_A is the efficiency of TL production from this dose. The average dose rate from the environment is d_B, with f_B being the corresponding TL efficiency. In general $f_A \approx f_B$.

The average dose per decay can be written as

$$D_A = \sum_i n_{Ai} \bar{E}_i \epsilon_i \quad . \qquad 9$$

The summation is over the i different particles emitted, and n_{Ai} being the relative abundance of the i^{th} particle whose mean energy is $\bar{E}_i$. The average fraction of this energy actually absorbed by the mass of the dosimeter is ϵ_i.

Because of the small size of TL dosimeters, only beta-rays contribute appreciably to the delayed dose. Most gamma- and x-rays escape without interacting. The ranges of the betas, tenths of millimeters, are not negligible compared to typical dosimeter dimensions either.

The absorbed fractions, ϵ_i, therefore depend on the shape and size of the dosimeter and on the amount of backscatter from the surroundings. For example, the measured delayed dose to a LiF extruded ribbon dosimeter, 3x3x1 mm, covered on its large faces by similarly activated dosimeters, is about 30% greater than delayed dose to an isolated single dosimeter. While it is impractical to surround dosimeters with similarly activated material and thus obtain the maximum delayed dose, providing a consistent backscatter geometry will insure reproducibility. The aluminum holders described in the annealing section provide this consistency.

Powder dosimeters require a consistent package geometry as well. Small gelatine capsules, consistently filled, are most convenient and inexpensive. Wrapping lead foil, 0.2 mm thick, around the capsule gives reproducible backscatter and excludes light. Still, the grains of phosphor near the outside receive less dose than those in the center. The capsule contents should be mixed carefully before samples are removed from readout. Fig. 8 shows dosimeters in their storage containers.

The accurate timing of the storage is not critical for most cases. The relative insensitivity of the measurement to variations in the storage time is an important advantage to the technique. It allows the delayed doses to be measured sequentially with one reader after the dosimeters themselves have integrated the doses in parallel.

For storage times greater than $4/\lambda_A, (6t_{1/2})$, less than 2% of the original activity remains. After this time the principal time dependent error sources are the fading of the TL signal and the uncertainty

Figure 8. Picture of the Neutron Activated Dosimeters Ready for Storage.

The Magnesium Silicate dosimeters are in the carrier at the left which has been covered with black tape to exclude light. The extruded ribbon samples are in the aluminum holder at the top right. The gelatine capsule lying on the lead foil at the bottom right contains about 100mg of Calcium Sulfate. The lead foil is wrapped around the capsule and stored with the axis vertical to insure consistent packing. The Zinc Oxide capsule is treated the same as the Calcium Sulfate and is indistinguishable from it at the resolution of this photograph, therefore not shown.


METRIC 1 2 3 4 5 6 7 8 9 10

in the amount of background radiation. The latter uncertainty grows roughly as $t^{1/2}$. The background itself can be measured using unactivated dosimeters annealled and stored together with the activated ones. This is the preferred method because the background internal to the dosimeter is required. This internal background varies with phosphor type. The LiF dosimeters measure about 1mR/day while the ZnO gives almost 15mR/day.

The fading depends on the type of phosphor and the storage temperature. The worst case among the phosphors used here is a 5% fading in the first day at room temperature observed for CaF_2:Mn.

The problem of optimizing the storage time for maximum TL signal is considered further in Appendix I. The storage times actually chosen are listed in Table II. The case of $CaSO_4$:Dy, reaction $^{32}S(n,p)^{32}P$, is special in that six half lives for ^{32}P (3 months) is generally too long to wait for data. Hence two weeks, one half life, is arbitrarily chosen in the trade off between maximum TL signal and patience. Another special feature of this phosphor is that the delayed dose from the ^{165}Dy which is activated primarily by thermal neutrons can be separated from the delayed dose from the ^{32}P activation. This is discussed in the analysis section of this chapter.

Readout: After the appropriate storage time, the delayed dose TL is measured with the TL reader described in the apparatus chapter. The dosimeters are handled in red safelight conditions since the TL phosphors all show some light sensitivity. Each dosimeter is heated at a linear rate of 8°C/sec to a maximum temperature of 400°C in a

TABLE II

Storage Times Appropriate to Each Phosphor

Phosphor	Nuclide	Storage Time
LiF:Mg,Ti	^{18}F	1 day
CaF_2:Dy	^{18}F, ^{165}Dy	1 day
CaF_2:Mn	^{18}F, ^{56}Mn	1 day
Mg_2SiO_4:Tb	^{24}Na	3 days
ZnO:Tm	^{64}Cu	3 days
$CaSO_4$:Dy	^{165}Dy	1 day
	^{32}P	14 days

helium atmosphere. After a total heating period of one minute which includes about ten seconds at 400°C, the heater and dosimeter cool at about 30°C/sec. A second heating cycle without moving the dosimeter is used to obtain the phototube dark counts and the incandescence from the heater and dosimeter which must be subtracted from the TL measured during the first heating.

The TL emitted from a dosimeter is not isotropic, especially from old, used dosimeters. Variations in light output of 10% have been observed by merely inverting the dosimeter. Dosimeters showing such large variations usually have some observable damage. Even in the absence of observable differences, the TL light output varies among dosimeters. Each dosimeter is therefore given a calibrating exposure to 100 mR of gamma-rays from a ^{137}Cs source. The readout of the calibrating exposure is essentially the same as for the delayed dose with the orientation of the dosimeter being reproduced as well as possible.

The dosimeters in powder form present handling problems. Small pans, approximately 12mm in diameter and 2mm deep of 0.1mm thick silver, hold the powder samples. As noted previously, the delayed dose is not uniform and the phosphor must be mixed carefully before the TL samples are taken out into the pans. The samples must also be spread evenly and thinly to avoid having the upper layers scatter the TL from the bottom grains out of the aperture of the phototube. In the silver pans used, the powder samples showed a TL proportional to mass up to about 50mg. Finer grained powders will show this TL reduction due to scattering at smaller masses. The normal sample size

in this study is 20 to 30 mg. A #5 gelatin capsule contains 5 or 6 such samples. The powder samples are left in their pan during the whole readout and calibration sequence. Fig. 9 shows the TL dosimeters after readout.

Analysis: The set of TL measurements must now be related to the neutron exposure. For the short exposure case, Eq. 8 can be rewritten as

$$TL(t_{ra}) = k\left\{\sum_A N_p\left[1-\exp(-\lambda_A t_{ra})\right] D_A f_A \int_0^{E_{max}} \sigma_A(E)\,\Phi(E)\,dE + d_B f_B t_{ra}\right\} . \qquad 10$$

A sensitivity function, S_A, can be defined for each dosimeter type and each activated nuclide.

$$S_A \equiv k N_p\left[1-\exp(-\lambda_A t_{ra})\right] D_A f_A . \qquad 11$$

In particular,

$$S_A(\infty) = k N_p D_A f_A . \qquad 12$$

which obtains for $t_{ra} > 6t_{1/2}$, to within 2%. Writing the TL from the background radiation as

$$B(t_{ra}) = k d_B f_B t_{ra} , \qquad 13$$

equation 10 can be restated as

Figure 9. Picture of the Dosimeters after Readout.

The glass-encapsulated Mg_2SiO_4:Tb dosimeter is seen at the left. The extruded chips in the center are: top, LiF (TLD-700), middle, CaF_2Dy (TLD-200), and bottom, CaF_2:Mn. The powder samples of $CaSO_4$:Dy at the top and ZnO:Tm at the bottom are shown in their silver pans at the right.

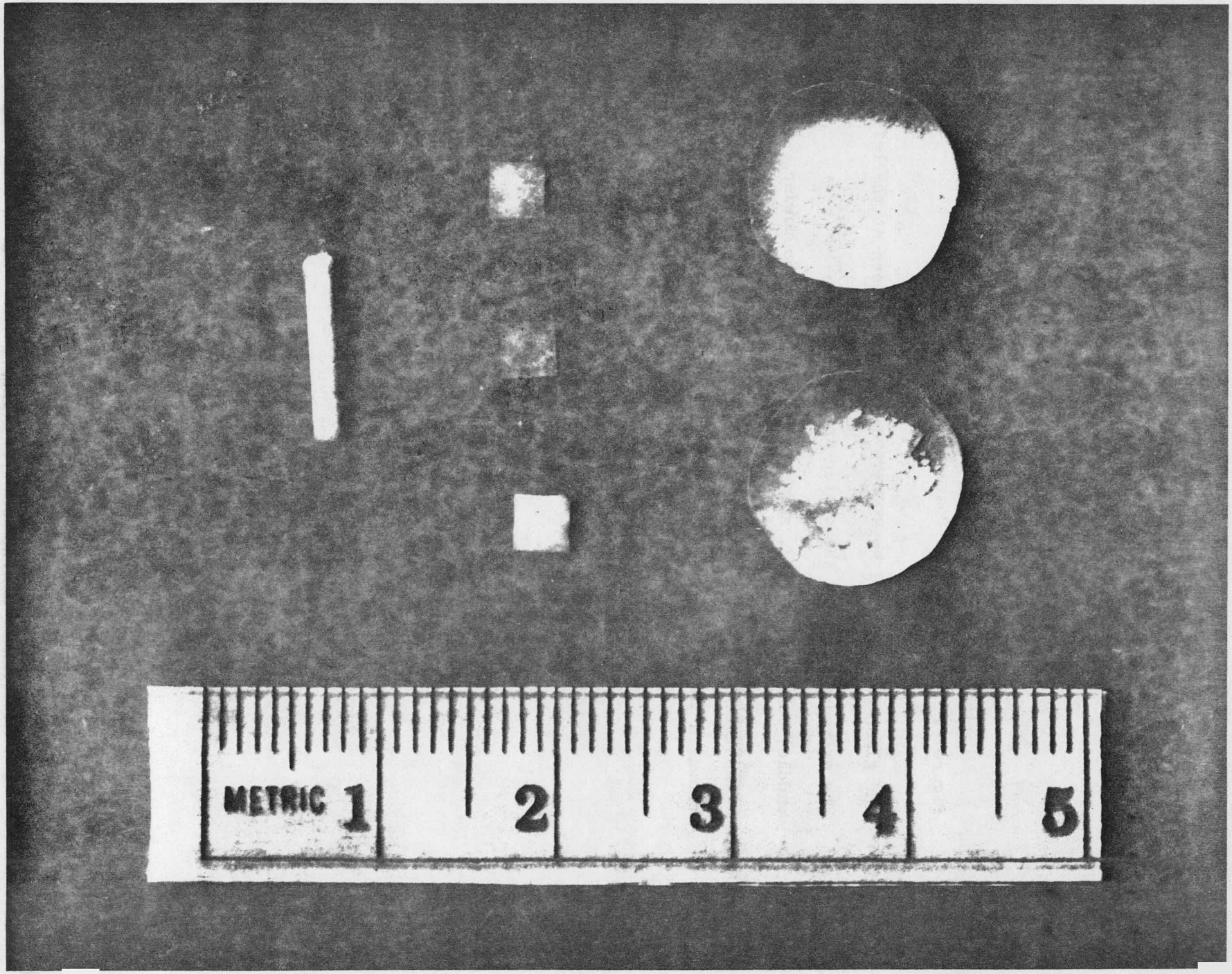
METRIC
1
2
3
4
5

$$TL(t_{ra}) - B(t_{ra}) = \sum_A S_A(t_{ra}) \int_0^{E_{max}} \sigma_A(E)\, \Phi(E)\, dE \,. \qquad 14$$

For the constant flux case, a similar equation can be written:

$$TL(t_{ra}) - B(t_{ra}) = \sum_A S_A(t_{ra}) \left[1 - \exp(-\lambda_A t_e)\right] \lambda_A^{-1} \int_0^{E_{max}} \sigma_A(E)\, \phi(E)\, dE \,. \qquad 15$$

In principal the sensitivity functions $S_A(t_{ra})$ can be calculated from Eqs. 11 and 9. However, the dependence of the absorbed fractions, ϵ_i, and the efficiency factors, f_A, on the condition of the individual dosimeter and its surroundings complicates this. Since reasonably monoenergetic neutron sources of adequate intensity are available, the $S_A(t_{ra})$ are more readily determined experimentally. The judicious choice of the neutron energy can reduce the summation in Eqs. 14 and 15 to a single term.

The sensitivity function $S_A(t_{ra})$ is measured by exposing the dosimeter to a known neutron fluence and measuring the delayed dose $TL(t_{ra})$. Given a monoenergetic source of energy E_n such that $\sigma_A(E_n)$ is known and the cross sections for other, competing reactions are essentially zero, Eq. 14 can be solved for the sensitivity:

$$S_A(t_{ra}) = \left[TL(t_{ra}) - B(t_{ra})\right] / \left[\sigma_A(E_n)\, \Phi(E_n)\right]. \qquad 16$$

Likewise for a constant flux source

$$S_A(t_{ra}) = \left[TL(t_{ra}) - B(t_{ra})\right] \lambda_A \Big/ \left\{\sigma_A(E_n)\, \phi(E_n) \left[1 - \exp -\lambda_A t_e\right]\right\} \,. \qquad 17$$

For the phosphors included in this study only 14 MeV and thermal neutron sources are required to measure the relevant sensitivity functions.

Once the sensitivities are known, one can solve Eq. 14 for the fluence or Eq. 15 for the flux from an unknown exposure. For dosimeters with a single activating nuclide, Eq. 14 can be written

$$(TL-B)/S = \int_0^{\bar{E}_{max}} \sigma(E)\, \Phi(E)\, dE . \qquad 18$$

For dosimeters with two activating nuclides, i and j, the summation in Eqs. 14 or 15 can be treated in different ways. If the half life of one is at least ten times the half life of the other, their activities can be measured separately by reading the TL at two different times. This is the case for the phosphor $CaSO_4$:Dy with activated nuclides ^{32}P, $t_{½}$=14 days and ^{165}Dy, $t_{½}$=140 mins. The first reading at time $t_{rai} > 6t_{½i}$ measures the delayed dose from almost all of the short lived nuclide i, plus a fraction $(1-\exp-\lambda_j t_{rai})/(1-\exp-\lambda_j t_{raj}) = F_{ij}$ of the long lived nuclide. The amount of long lived nuclide j is determined from a subsequent delayed dose measurement at time t_{raj}.

For the long lived nuclide j at the time t_{raj},

$$TL(t_{raj}) - B(t_{raj}) = (1-F_{ij})\, S_j(t_{raj}) \int_0^{\bar{E}_{max}} \sigma_j(E)\, \Phi(E)\, dE . \qquad 19$$

The TL from the short lived nuclide i can then be found from the delayed dose measured by the first reading at time t_{rai} from

$$TL(t_{ra_i}) - B(t_{ra_i}) - F_{ij} S_j(t_{ra_j}) \int_0^{E_{max}} \sigma_j(E) \Phi(E) dE = S_i(t_{ra_i}) \int_0^{E_{max}} \sigma_i(E) \Phi(E) dE. \quad 20$$

These equations can be put into the form of Eq. 18:

$$(TL-B)/(1-F)S = \int \sigma \Phi \quad , \quad 21$$

and

$$(TL-B-FQ)/S = \int \sigma \Phi \quad 22$$

where Q is the contribution to the first delayed dose measurement from the longer lived nuclide.

If the decay half lives of the two nuclides are similar, no separation of their contributions to the delayed dose can be made. In this case an effective cross section and an effective sensitivity can be defined. The effective cross section is given by

$$\sigma_{eff}(E) = \frac{S_i(t_{ra})}{S_j(t_{ra})} \sigma_i(E) + \sigma_j(E) \quad , \quad 23$$

and the effective sensitivity is $S_j(t_{ra})$. One can again write an equation in the form of Eq. 18:

$$(TL-B)/S_{eff} = \int \sigma_{eff} \Phi \quad . \quad 24$$

Thus the delayed dose TL measurements from any set of dosimeters can be expressed in the form of Eq. 18. Techniques for unfolding the

neutron spectrum from such a set of equations have been developed for conventional activation detectors which can be directly applied. The report by Routti (reference 9, Chapter I) contains an explanation of these techniques.

CHAPTER IV

EXPERIMENTAL APPARATUS

TL Reader: Since the delayed dose TL is quite small, typically a millirad for a neutron fluence which delivers a few rads to tissue, the TL reader must have a sensitive and stable light detection system and a highly reproducible heating system. The reader we use is basically a commercial instrument* modified as described below. The basic design of a TL reader is diagrammed in Fig. 10.

Photomultiplier tubes are the most sensitive light detectors available. The anode output of a photomultiplier tube (PMT) at low light levels consists of a series of current pulses which originate as individual electrons mostly from the photocathode with some coming from the dynodes. Usually these pulses are summed and averaged to give an anode current. Measurement of the anode current cannot distinguish the true photocurrent from other sources such as leakage and dynode current. Moreover, anode current depends on the gain of the PMT which is related to some large power, 7 to 10, of the operating voltage. Thus small variations in the applied voltage cause large variations in the PMT gain and measured anode current.

For low light levels, the most sensitive and stable detection technique is to count the photons.[1] With photon counting, only the anode pulses larger than some threshold value are counted. The threshold is set to discriminate against leakage currents and the smaller

---

* Model 2000A, Harshaw Chemical Company, Solon, Ohio.

Figure 10. Block Diagram of the TL Reader.

The START signal turns on a linear voltage ramp. This ramp voltage and an amplified thermocouple voltage proportional to the heater temperature are compared to obtain a control signal for the heater power. The sensing thermocouple which is spot welded to the heater strip is referenced to the PMT housing cooled by the thermoelectric cooler. The heater strip is mounted in a light tight drawer which opens to replace the dosimeter. The continuous He gas flow eliminates the oxygen dependent spurious luminescence and improves the thermal contact between the dosimeter and the heater strip.

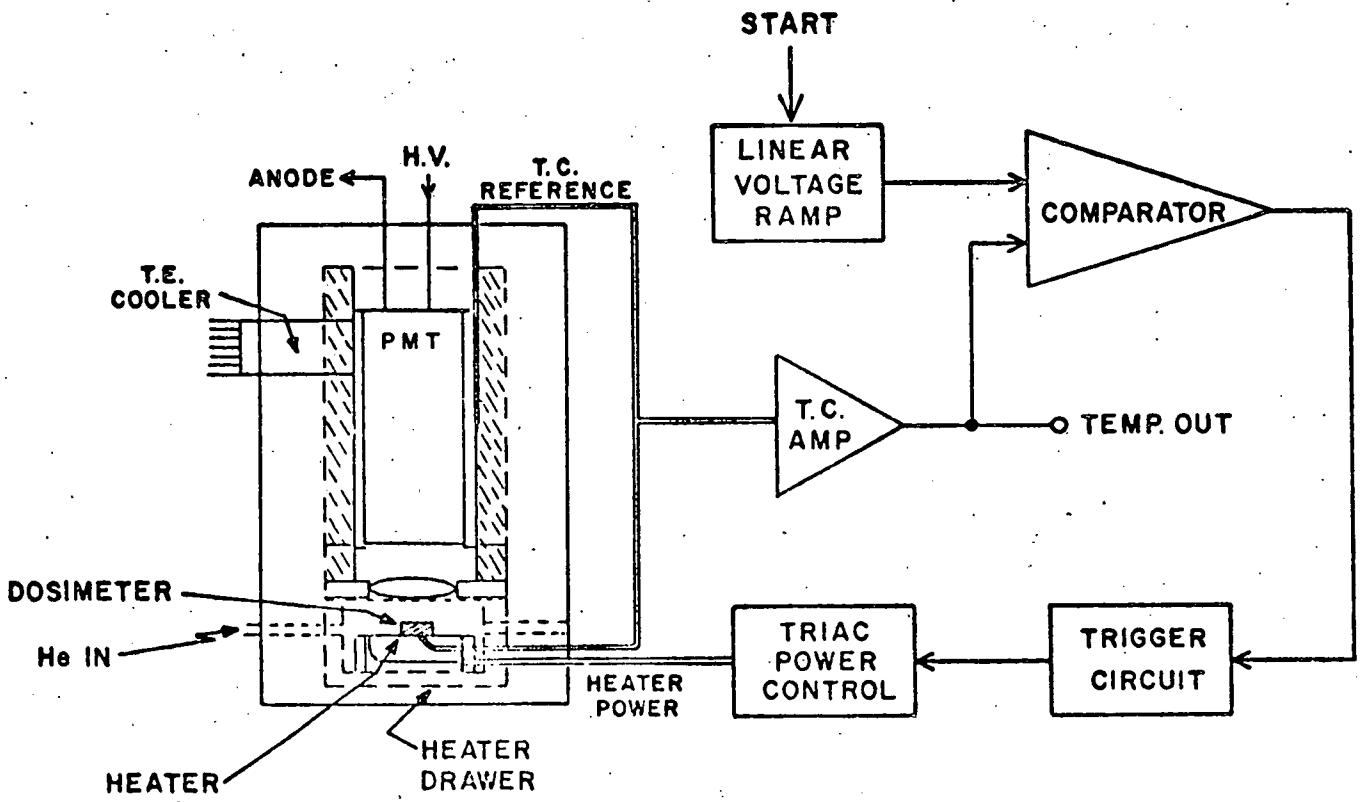
START
LINEAR VOLTAGE RAMP
COMPARATOR
ANODE
H.V.
T.C. REFERENCE
T.E. COOLER
PMT
T.C. AMP
TEMP. OUT
DOSIMETER
He IN
TRIAC POWER CONTROL
TRIGGER CIRCUIT
HEATER POWER
HEATER DRAWER
HEATER

pulses which originate on the dynodes. Extremely large pulses from scintillations or discharges do not contribute excessively as they would with a current measuring technique. An upper level discriminator is not required. Excellent long term stability is achieved because any variation in PMT gain or discriminator level affects only that small fraction of pulses whose amplitudes are near the discriminator level.

To facilitate the pulse height discrimination, the voltage between the photocathode and first dynode is stabilized at 300V with zener diodes to give the maximum first stage gain. These zeners must be capacitively bypassed to eliminate noise. The rest of the voltage divider string is arranged and capacitively stabilized for pulse mode operation. The dark current (dark count rate) is reduced by cooling the PMT to about 0°C with a thermoelectric cooler.

The platinum heater strip is heated at a linear rate by a controlled ac current. The high frequency electronic noise normally associated with the triac controller is suppressed with bypass capacitors. The feedback for the heater controller is obtained from a thermocouple spot welded to the platinum strip. An amplified signal from this thermocouple referred to the 0°C PMT cooler, appears as the "temperature out" signal which is used to control the counting electronics.

To improve the thermal contact between the heater and the sample, the sample chamber is flushed with helium gas. An inert gas atmosphere is required to suppress spurious luminescence.[2] Helium has

the additional advantage of speeding the cooling of the heater and dosimeter, shortening the readout cycle by about thirty per cent.

Counting Electronics: A diagram of the whole reader system is shown in Fig. 11. A commercial photon counting amplifier/discriminator* is connected to the PMT anode output. The discriminator level is set to the manufacturers specifications. An external attenuator positions this level between the noise and photocathode originated pulses.

A standard pulse is generated for each anode pulse greater than the discriminator level. These are counted with a scaler of our own design based on the type 74192 decade counters. System counting rates up to 1MHz have been measured with losses of less than 2% by the two source technique. The two light sources were tritiated organic scintillators. To obtain visual display of the glow curve, the pulses also are prescaled and stored in the memory of a multichannel scaler.** The contents of this memory can be displayed on a CRT, typed out, or plotted on an X-Y recorder.

The portion of the glow curve to be counted is selected by a double comparator which compares the "temperature out" voltage with two presetable reference voltages and generates an enable pulse which gates the scaler. The scaler can count up or down. The count down feature is used to subtract dark counts and incandescence during a second heating. Marker pulses at the beginning and end of the enable pulse are sent to the multiscaler for visual reference.

---

* Model 1120 SSR Instruments Company, Santa Monica, California.

** Nuclear Data Model 120, Nuclear Data Inc., Schaumburg, Illinois.

Figure 11. Block Diagram of the Photon Counter

The START signal begins the TL reader heating cycle and the multichannel scaler sweep. The PMT ANODE signal is processed by the preamp-discriminator to give standard pulses proportional to the number of photons incident. The PHOTON COUNTS are prescaled to reduce the count rate and recorded in the multichannel scaler. The temperature comparator generates an ENABLE signal which opens the signal gate to the scaler between the temperatures selected for integration of the TL. (These temperatures were indicated by the arrows on the glow curves shown in Chapter I.)

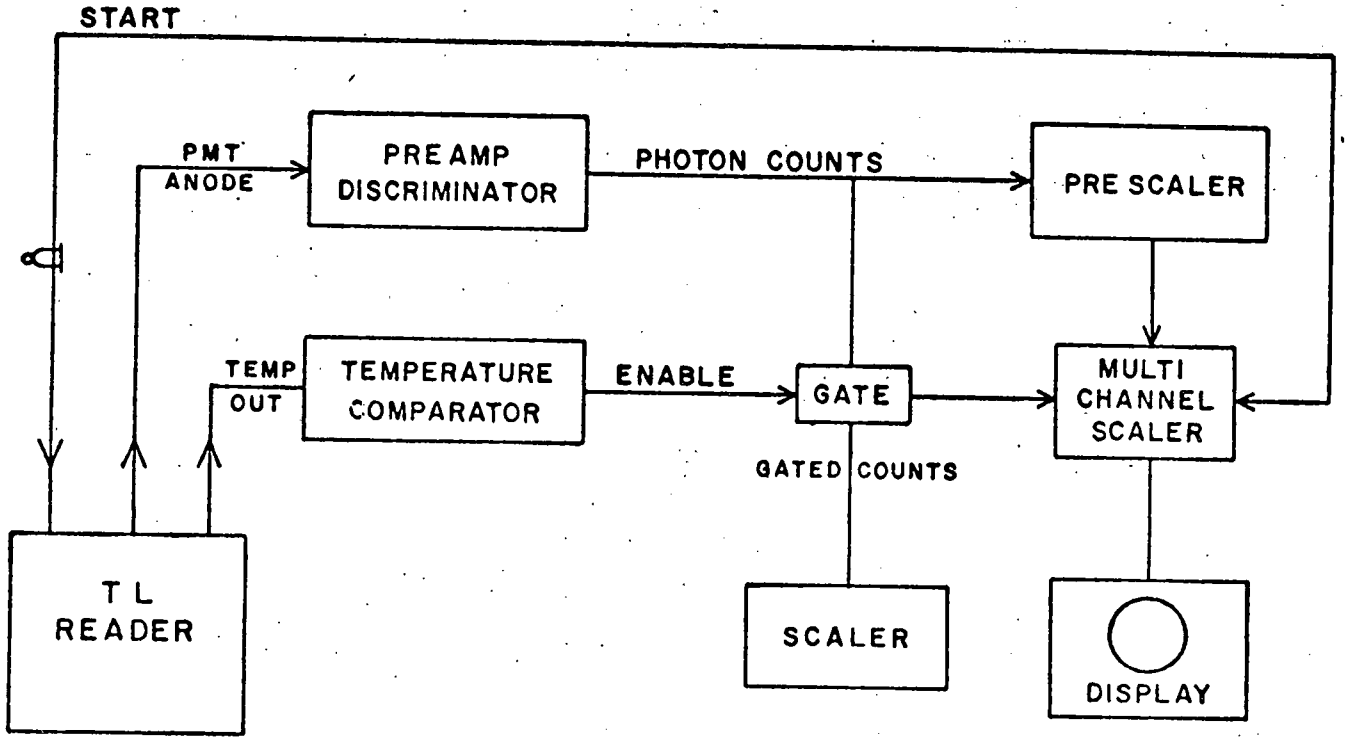
START
PMT
ANODE
PREAMP
DISCRIMINATOR
PHOTON COUNTS
PRE SCALER
TEMP
OUT
TEMPERATURE
COMPARATOR
ENABLE
GATE
MULTI
CHANNEL
SCALER
GATED COUNTS
T L
READER
SCALER
DISPLAY

Fast Neutron Source: The fast neutrons were supplied by a commercial neutron generator.* This machine accelerates deuterons to a maximum energy of 200 KeV at a copper backed, thick, titanium tritide (TiT) target 2 cm in diameter. The reaction $^{3}H(d,n)^{4}He$, (D-T), produces neutrons of approximately 14.7 MeV, cleverly called 14 MeV neutrons. The reaction $^{2}H(d,n)^{3}He$, (D-D), gives neutrons of about 3 MeV from a TiD target. The characteristics of neutron generators of this type are discussed in detail by Nargolwalla and Przybylowicz.(3)

With an accelerating potential of 200 kV and a beam current of 2 mA, about 10^{11} n/sec are produced from a new TiT target. Under these conditions, the neutron output drops to one half in 20 to 30 minutes. A relatively constant flux can be maintained by starting with a lower beam power and increasing it as the target efficiency drops. A flux of the order of 10^{8} n/(cm^{2}min) can be maintained 10 cm from the target for at least 30 mins. The production rate for neutrons from the D-D reaction is two orders of manitude smaller. Since the deuteron target is constantly being replenished, the 3 MeV neutron flux can be maintained reasonably constant for long times.

The "14 MeV" neutrons from the D-T reaction actually range in energy from 14 MeV to 15 MeV. This energy spread has several sources. The TiT target is thick so that all deuteron energies up to the maximum are present. With a beam diameter of 2 cm all reaction angles up to about 10° are present for the geometry used.(4) The target assembly itself is a scattering source, with up to 40% of the neutrons being

---

* Activatron Model 211 M, Accelerators, Inc., Austin, Texas.

scattered in some configurations.[5] In addition, the build-up of deuterons in the target from the incident beam results in the appearance of a few 3 MeV neutrons.

The 14 MeV neutron fluences used in this study were calibrated with conventional activation techniques using the reactions $^{19}F(n,2n)^{18}F$, $^{63}Cu(n,2n)^{62}Cu$ and $^{32}S(n,p)^{32}P$.[6] The 511 keV annihilation quanta from the positron decay of the ^{18}F and ^{62}Cu nuclides were counted with a NaI:Tl well-counter. The well-counter was calibrated with a ^{22}Na standard source. The ^{32}P activity was concentrated by burning off the remaining sulfur and was counted with a thin window G-M tube. The G-M tube was calibrated with a ^{32}P standard source. When exposed to the same neutron fluence, measurement of these three nuclides gave calculated fluences which agreed to within ten per cent. This good agreement reflects to some extent a fortuitus choice of cross sections.

Only the $^{32}S(n,p)^{32}P$ reaction is possible with 3 MeV neutrons. The choice of cross section in this energy range is particularly difficult due to the strong energy dependence exhibited and the wide disparity among published values.[7]

Manual control of the deuteron beam was used to maintain a nearly constant neutron flux. Two systems were used to monitor the instantaneous flux. A neutron rem meter* was located about two meters from the target at about 100° from the beam direction. The ratemeter output from this detector was used as the main flux monitor. The sensitivity of this detector to scattered neutrons however, limited its value as

---

* Texas Nuclear Model, Nemo 9140, Texas Nuclear Inc., Austin, Texas.

a calibration system. The output from a plastic scintillator* located one meter from the target on the beam axis provided run to run comparison.

Thermal Neutron Source: Thermal neutron exposures were obtained in the "tortoise tube" facility of the UW nuclear reactor. This facility accesses the graphite thermal column for neutrons with a cadmium ratio greater than 10^3. The thermal flux is specified as 8.4×10^8 nvt at the rated power of one megawatt as measured by activation of calibrated gold foils. Exposures of two minutes give a fluence of 1.14×10^{10} n/cm^2.

Fission Neutron Source: Fast neutrons with an energy distribution approximately that of a fission spectrum are available at the number 4 beam port of the UW nuclear reactor. A pipe approximately 15 cm inside diameter extends through the concrete shield from a point 7.6 cm from the TRIGA core. The space between the core edge and the beginning of the beam port pipe is filled with an aluminum clad bismuth reflector. The thermal neutrons which leak through the bismuth reflector are further reduced by a 1.6 cm thick boral plate in the beam tube. Contamination of the emerging fast neutron beam with gamma-rays is reduced with 9.2 cm of lead. The beam port tube terminates outside the shield in a steel drawer assembly backed by a large water filled tank. An irradiation region approximately 25 cm square and 40 cm along the beam axis at the end of the beam tube is accessible through the steel drawer.

---

* NE 213, Nuclear Enterprises Inc., San Carlos, California.

The fast neutron beam in this region has a reasonably uniform flux over its 15 cm diameter cross section. A uniform background of scattered neutrons fills the entire irradiation region. The fast neutron flux rate is about 4×10^{10} n/cm^{2}hr assuming a fission like energy distribution at the rated power of 1 megawatt.

Gamma-ray Source: A ^{137}Cs gamma-ray source of about 70 mCi was used for the TL calibrating exposures. Exposure rates, calibrated against a cobalt standard source, of 1 mR/min and 10 mR/min were used. Exposures of 10 mR or 100 mR could be reproduced with a standard deviation of ½%.

REFERENCES

1. M. J. Aitken, J. C. Alldred and J. Thompson, CONF 680920, P. 248, (1968). Clearinghouse for Federal Scientific and Technical Information, Springfield, VA 22151.

2. V. Svarcer and J. F. Fowler, CONF 650637, P. 227, (1967). Clearinghouse for Federal Scientific and Technical Information, Springfield, VA 22151.

   M. J. Aitken, J. Reid, M. S. Tite and S. J. Fleming, ibid., P. 236.

3. S. S. Nargolwalla and E. P. Przybylowicz, Activation Analysis with Neutron Generators, Wiley, NY, (1973).

4. J. B. Marion, "Neutron Production with Dynamitron and Dynagen Accelerators," Radiation Dynamics, Inc., Westbury, NY, (1961).

5. E. Ricci, J. Inorg. Nucl. Chem. 27, 41, (1965) discussed in S. S. Nargolwalla and E. P. Przybylowicz, Activation Analysis with Neutron Generators, P. 244, Wiley, NY, (1973).

6. ASTM, E261, E265, Part 31, Book of ASTM Standards, ASTM, Philadelphia, PA, (1966).

7. J. J. Broerse, Effects of Energy Dissipation by Monoenergetic Neutrons in Mannalian Cells and Tissues, Radiobiological Institute TNO of the Organization for Health Research, TNO, Rijswijk, Netherlands, (1966).

CHAPTER V

MEASUREMENT OF THE SENSITIVITY FUNCTIONS

As was mentioned in Chapter III, the sensitivity functions, $S_A(t)$, are more easily measured experimentally than calculated. Both the delayed dose absorbed and the efficiency with which the TL is produced and emitted are difficult to calculate. This chapter describes the measurement of the TL efficiency of the individual dosimeters and the neutron activation sensitivity of the dosimeter types listed in Table III. These measured sensitivities are applicable, however, only to dosimeters of the same composition and geometry.

The activity induced by a neutron exposure depends only on the composition of the dosimeter, that is the number and kind of precursor or parent nuclei. The delayed dose produced by this activity depends on the geometry of the dosimeter and the backscatter from the dosimeter holder. The composition and geometry are determined during manufacture to high precision for solid dosimeters. The backscatter also can be readily reproduced by using a standard holder. For powder phosphors, the geometry of the container used during storage must be standardized, for example by using a number 5 gelatin capsule filled consistently. These factors all can be reproduced with precisions of one per cent, thus the delayed dose itself can be very reproducible.

However, the TL light output efficiency for a given delayed dose depends on the optical properties of the individual dosimeters. Surface scratches, dirt, metallization from handling with forceps and prior radiation exposures all affect the efficiency with which the TL

TABLE III

Description of the Dosimeters

Phosphor	Mass	Shape
LiF:Ti,Mg	23 mg	3.2 x 3.2 x 1 mm; extruded ribbon
CaF_2:Mn	50 mg	3.3 x 3.3 x 2.5 mm; hot pressed chip
CaF_2:Dy	27 mg	3.2 x 3.2 x 1 mm; extruded ribbon
Mg_2SiO_4:Tb	20 mg	2 mm diam x 10 mm; glass capillary encapsulated, 30 mg of glass
ZnO:Tm	180 mg	4 mm diam x 10 mm; ungraded powder and small crystallites in a #5 gelatin capsule
$CaSO_4$:Dy	180 mg	4 mm diam x 10 mm; 80 mesh powder in a #5 gelatin capsule

is produced and emitted.[1] Powder samples also show variations due to differences in sample mass and distribution.[2] Precision measurement thus requires that each individual dosimeter be calibrated. The delayed dose is primarily from uniformly distributed beta emitters; therefore gamma-rays, which produce a uniform internal flux of electrons are a convenient radiation source to determine the TL efficiency of the individual dosimeters.

Individual Dosimeter TL Efficiencies: The net number of TL photons detected for an exposure of 10 mR of ^{137}Cs gamma-rays was averaged for 10 to 20 individual dosimeters of each phosphor type. The average value for each phosphor type was rounded to two significant figures and the TL efficiency for the individual dosimeters calculated with respect to this average value. Measurements of successive exposures agreed well if the orientations of the dosimeters was reproduced during each readout. Table IV gives the average TL efficiency and the reproducibility (standard deviation) for successive exposures to an individual dosimeter. The powder sample efficiencies are given per mg. The TL output is proportional to powder mass up to about 40 mg for the grain sizes used. The PMT used has an S-11 response and was used without any color filters. The estimated light detection efficiency is about 1%.

Fast Neutron Activation Sensitivities: The fast neutron activation sensitivity $S_A(t)$ was calculated from the measured delayed dose TL corrected for individual dosimeter efficiency, following activation

TABLE IV

Gamma-Ray TL Sensitivities

Phosphor	Gamma Response TL Photons/mR	10 mR Exposures
LiF	400	4 %
CaF_2:Mn	1.0×10^4	2 %
CaF_2:Dy	2.7×10^4	1.3 %
Mg_2SiO_4:Tb	2.0×10^4	5 %
ZnO:Tm	2.8×10^3/mg	6 %
$CaSO_4$:Dy	4.5×10^3/mg	5.5 %

with a known fluence of 14 MeV neutrons. For a monoenergetic neutron fluence $\Phi(E_n)$ of a particular neutron energy E_n such that $\sigma_A(E_n)$ is well known and the cross sections at that energy for all of the other important reactions are essentially zero, the sensitivity can be calculated from

$$S_A(t_{ra}) = [TL(t_{ra}) - B(t_{ra})] / [\sigma_A(E_n)\,\Phi(E_n)] \,. \qquad 25$$

The expression $[TL(t_{ra})-B(t_{ra})]$ is the net number of TL photons counted from the delayed dose, normalized to the average TL efficiency given in Table IV.

Dosimeters of each of the phosphor types along with one gram of LiF to monitor the fluence by conventional activation techniques, were exposed for ten minutes to 14.7 MeV neutrons from the D-T neutron generator. The dosimeters were arranged to occupy a disk approximately 2 cm in diameter, whose plane was parallel to the plane of the target, at a distance of 10 cm in the forward direction. The nearest scattering source for neutrons (except for the target assembly itself) was the concrete floor about one meter away. Neutrons with energies from 14 to 15 MeV were present with the median energy taken to be 14.7 MeV. The fluence during the 10 min exposure was calculated from the $^{18}_{7}$ activity induced in the one gram LiF sample as measured with a calibrated NaI:Tl well-counter. Taking the effective cross section for the fluorine activation to be 65 mb,[3] the fluence was $2.2 \times 10^9 n/cm^2$.

The exposed dosimeters were annealed at 500°C for five minutes along with a similar set of unexposed dosimeters. Ten minutes after

the end of the exposure all the dosimeters had been annealed and returned to their holders at room temperature. Correction was made for the loss of activity during this ten minute interval.

Twenty hours later, the TL from the delayed dose to the LiF, CaF_2 and $CaSO_4$ dosimeters was measured. The ZnO and Mg_2SiO_4 dosimeters were read 70 hours after the exposure. Fourteen days after the exposure the $CaSO_4$ dosimeters were measured again (thirteen days had elapsed since the first readings). The unexposed dosimeters were measured at the appropriate times to obtain the TL contribution from the background radiation environment. The TL efficiency of each dosimeter was remeasured using a 10 mR gamma-ray exposure after its delayed dose had been read. The measurements of the TL from delayed dose and background was corrected for the individual dosimeter efficiency. Eq. 25 was then used to calculate the fast neutron sensitivities from these measurements using the neutron cross sections listed in Table V.

Thermal Neutron Activation Sensitivities: To determine the thermal neutron sensitivities of the dosimeters, several of each phosphor were exposed in the UW nuclear reactor thermal column. A two minute exposure in the tortoise tube gave a fluence of $1.14 \times 10^{10} n/cm^2$.

The exposed dosimeters were annealed along with a similar set of unexposed dosimeters for 5 minutes at 500°C. Fifty minutes after the end of the exposure all of the dosimeters were integrating the delayed dose from the thermal neutron induced activity.

The delayed dose TL was measured after one day (23 to 25 hours), for all the dosimeters except ZnO:Tm. For the LiF and CaF_2 dosimeters,

TABLE V

Neutron Activation Sensitivities

Dosimeter	$S(t_r)$ Thermal $\frac{\text{TL Photons}}{\text{barn n/cm}^2}$	σ(th)	$S(t_r)$ 14.7 MeV $\frac{\text{TL Photons}}{\text{mbarn n/cm}^2}$	σ(14.7 MeV)	t_r
LiF:Mg,Ti	--	--	$3.3 \pm 0.3 \times 10^{-9}$	65 mb	1 day
CaF_2:Mn	$1.08 \pm 0.03 \times 10^{-5}$	13 b	$3.9 \pm 0.1 \times 10^{-7}$	65 mb	1 day
CaF_2:Dy	$2.1 \pm 0.14 \times 10^{-7}$	2.8 kb	$1.14 \pm 0.05 \times 10^{-6}$	65 mb	1 day
Mg_2SiO_4:Tb	$2.0 \pm 0.2 \times 10^{-5}$	.535 b	$7.2 \pm 0.3 \times 10^{-7}$	175 mb	3 day
ZnO:Tm *	$9.6 \pm 0.8 \times 10^{-8}$	1 b	$1.6 \pm 0.2 \times 10^{-7}$	200 mb	3 day
$CaSO_4$:Dy *	$9.1 \pm 0.4 \times 10^{-9}$	2.8 kb **	$1.4 \pm 0.1 \times 10^{-8}$	210 mb	14 day

* These are per mg values.

** The readout time for the thermal sensitivity is one day.

one day is the appropriate storage time for both fast neutron and thermal neutron activations. Standardization of the storage time simplifies the correction for TL fading.

The "one day" TL signal for $CaSO_4$:Dy measures all of the dysprosium decay dose and 5% of the potential dose from the decay of any ^{32}P present. For a thermal neutron exposure, no ^{32}P is produced in $CaSO_4$ so the one day TL measures only the dysprosium dose.

The Mg_2SiO_4:Tb dosimeters would normally be read after three days, both for thermal neutron and fast neutron exposures. A three day storage time accumulates 97% of the potential dose from the ^{24}Na radionuclide. However, to be certain that the observed thermal neutron sensitivity was in fact due to the activation of sodium in the glass capillary, these dosimeters were read at 23 hours and again at 49 hours after annealing. For ^{24}Na with a half life of 15 hours, the first reading should measure 65.5% of the potential dose and the second reading should measure an additional 24% leaving about 10% undecayed. The measured values of the TL at 23 hours and 49 hours were 66.5% and 24% respectively assuming 10% is undecayed. This agreement is well within experimental error. While the amount of sodium in the glass remains unknown, the thermal neutron sensitivity of the dosimeter is completely determined.

The ZnO:Tm dosimeters were read after three days. This is not the optimum storage time for the observance of a 57 minute half life isotope. However, the delayed dose TL should still be there although the background dose is higher than optimum. Three days is the standard storage time for fast neutron activation and information on the thermal

neutron sensitivity of this phosphor is useful in evaluating it as an error source in the dosimetry of fast neutrons rather than as a useful activation for measuring thermal neutrons.

The TL measurements of the delayed and background doses were corrected for the individual dosimeter efficiencies and for the fifty minute interval between the end of the exposure and the end of the annealing. Eq. 25 was then used to calculate the thermal neutron sensitivities from these measurements using the cross sections given in Table V.

The neutron energy dependence of activation detectors is entirely specified by the cross section. The cross sections are not particularly well known but their relative shapes as a function of neutron energy are somewhat more believable. The neutron energy response of the TL dosimeters can be given as the product of the sensitivity S and the cross section $\sigma(E)$. Fig. 12 is a plot of $S\,\sigma(E)$ for the dosimeters studied. The curves are the energy dependence of $\sigma(E)$ normalized to the measured value of $S\,\sigma(14.7)$ or $S\,\sigma(\text{thermal})$. The units are TL photons counted per incident $10^7 n/cm^2$ for the standard storage times given in Table II.

Figure 12. Sensitivity Functions $S\sigma(E_n)$ for the Dosimeters

These curves are essentially the effective activation cross sections normalized to the dosimeter sensitivities at 14.7 MeV and thermal neutron energies. The curves for CaF_2:Mn and ZnO:Tm are shown discontinuous since the cross sections considered all go to zero in the intermediate energy region. The fluorine cross section was taken from UK Library NDL 1972.[3] The magnesium cross section is from BNL 325.[4] The sulfur cross section is from the measurement of Allen, et al.[5] The zinc cross section has the shape calculated by Ringle[6] normalized to the measured values given in BNL 325.[4]

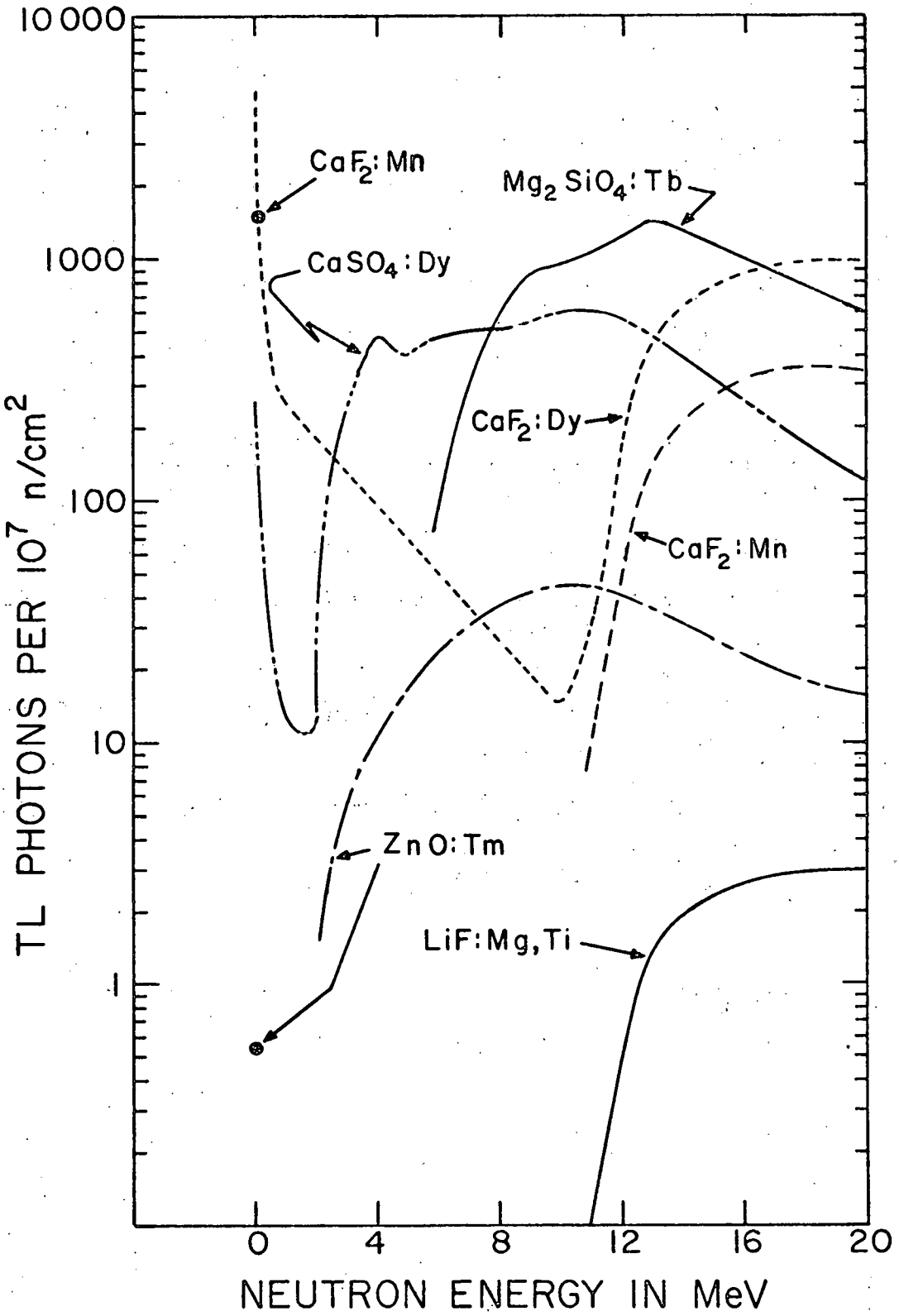
10 000
1000
100
10
1
TL PHOTONS PER 10^7 n/cm^2
CaF_2: Mn
Mg_2SiO_4: Tb
$CaSO_4$: Dy
CaF_2: Dy
CaF_2: Mn
ZnO: Tm
LiF: Mg, Ti
0
4
8
12
16
20
NEUTRON ENERGY IN MeV

REFERENCES

1. F. M. Cox, R. A. Arnold and B. M. Fabry, Paper, P. 161, 18th Annual Meeting of the Health Physics Society, 17-21, June, 1973.
2. G. W. R. Endres, CONF 650637, P. 435, (1967). Clearinghouse for Federal Scientific and Technical Information, Springfield, VA 22151.
3. Neutron Data Library, NDL 1972, United Kingdom Atomic Energy Authority, Harwell, U. K.
4. Neutron Cross Sections, BNL 325, 2nd ed. Superintendent of Documents, U. S. Government Printing Office, Washington, D. C. 20402.
5. L. Allen, Jr., W. A. Biggers, R. J. Prestwood and R. K. Smith, Phys. Rev. 107, 1363, (1957).
6. J. Ringle, UCRL 10732, U. of Cal. Rad. Lab., Berkeley, CA, (1963).

CHAPTER VI

EXPERIMENTAL MEASUREMENTS

Several experiments demonstrate the usefulness of the delayed dose technique. First, to be certain the activations produced were those listed in Table I, the half life of the induced activity was determined for the LiF and Mg_2SiO_4:Tb phosphors. Second, to characterize the spectrum of fission neutrons from the UW reactor, the dosimeters were exposed in the number 4 beam port. Third, the attenuation of 14.7 MeV neutrons by polyethylene was measured by the delayed dose in LiF dosimeters.

Decay Half Life: The decay half life can be determined from the time dependence of the delayed dose TL signal in several ways. If the activity is great enough, one can simply measure the activity directly as the delayed dose TL signal produced during a short time interval, say ten minutes: $\Delta TL/\Delta t=A$. Then one has at different times t,

$$\Delta TL(t)/\Delta t \propto \exp-\lambda t \,. \qquad 26$$

This method can be applied even to a multicomponent decay.

If the activity is insufficient to give an accurately measurable TL signal in a short time, the delayed dose can be read after several longer time intervals and fit to the expression

$$TL(t_{12}) = TL(\infty)\left[\exp-\lambda t_1 - \exp-\lambda t_2\right], \qquad 27$$

where t_{12} is the time interval t_2-t_1 between the first and second readings measured from the end of the activation and TL(∞) is the total potential delayed dose. This method is useful only for single component decays, and was used to confirm the activation of sodium as the thermal neutron reaction in the Mg_2SiO_4:Tb dosimeters discussed in Chapter V.

A slight modification of the latter method in which $t_2 \approx \infty$ demonstrates that the only significant radionuclide produced in the LiF:Mg,Ti phosphor is ^{18}F. Twenty extruded ribbon dosimeters were exposed to a fluence of approximately 10^{10} n/cm^2 of 14.7 MeV neutrons. All were annealed together for five minutes at 500°C. The dosimeters were divided into five groups of four each. The delayed dose TL of each group was measured twice, first at a time t_1 after the annealing and again at about 23 hrs post anneal. The times used as t_1 were ½, 1, 2, and 6.4 hours. The 23 hour reading was used to determine TL(∞). The dosimeters were individually calibrated with 100 mR exposures to ^{137}Cs gamma-rays. The activity remaining after a time t_1 is given by

$$TL(>t_1) = TL(\infty) \exp -\lambda t_1 \quad . \qquad 28$$

Fig. 13 is a plot of the delayed dose measured at 23 hours as a function of t_1. The line has a slope corresponding to a half life of 110 minutes, that of ^{18}F.

Similarly, the delayed dose remaining in the Mg_2SiO_4:Tb dosimeters was measured for t_1 times of 10, 14, and 27 hours. The second readout was at 108 hours post anneal. The data with two dosimeters in each

Figure 13. Delayed Dose Decay for LiF (TLD-700).

Each point represents the average TL from four dosimeters. The error bars are the standard deviations of the readings. The solid line corresponds to a decay half life of 110 min, that of ^{18}F.

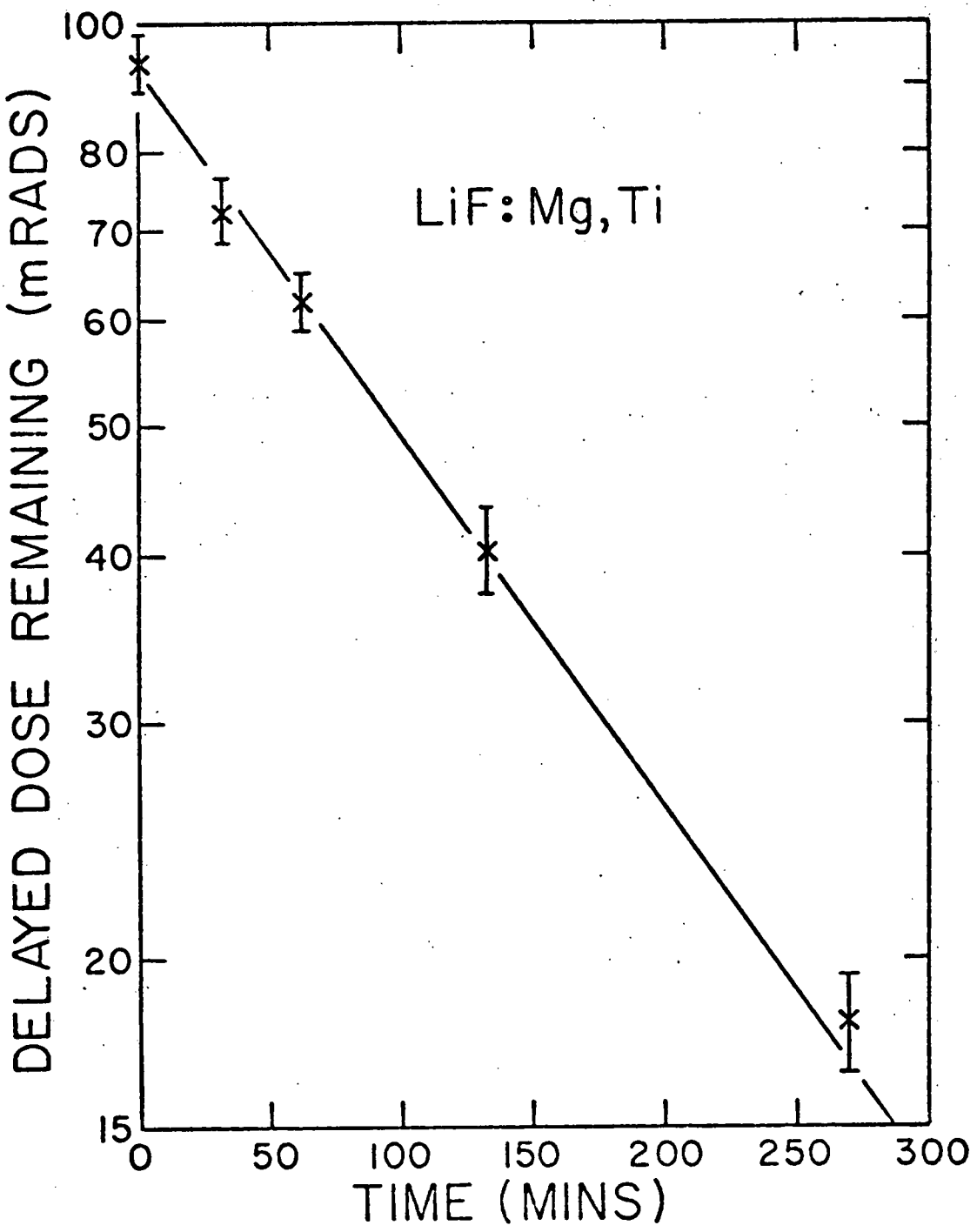
100
80
70
60
50
40
30
20
15
0
50
100
150
200
250
300
DELAYED DOSE REMAINING (mRADS)
TIME (MINS)
LiF:Mg,Ti

group are plotted in Fig. 14. The line has a slope corresponding to the half life of ^{24}Na, $t_{1/2}$=15 hours.

The phosphor $CaSO_4$:Dy was studied by Mayhugh and Watanabe[1] and a decay curve for activation by fission neutrons is given. The ^{165}Dy and ^{32}P components are easily resolved (see Fig. 15).

Fission Neutrons: In the course of dosimetry of the fast neutron flux from the number 4 beam port of the UW nuclear reactor for a radiobiological experiment, two groups of TL dosimeters were exposed to evaluate their delayed dose response. The neutrons have essentially an unmoderated fission spectrum from the TRIGA core with a background of thermal neutrons from the water beam stop. There is a well defined, circular, fast neutron beam in the sample area with the intensity in the surrounding penumbra being about 30 times less as measured with sulfur activation and a tissue equivalent ion chamber.[2] The thermal neutron background is essentially the same in the beam and penumbra. A thirty minute exposure gives a fission spectrum fluence of 2.1×10^{10} n/cm^2 at the beam center and 7×10^{8} n/cm^2 in the penumbra as measured by sulfur activation taking $\overline{\sigma}_{fission}$=65mb.[3]

Packets containing 4 CaF_2:Dy, 2 Mg_2SiO_4:Tb, 1 $CaSO_4$:Dy and 1 ZnO:Tm dosimeters were exposed for thirty minutes in the center of the fast neutron beam and in the penumbra. A third similar packet was kept for background measurements during the delayed dose accumulation. All three packets were annealed together for five minutes in the 510°C furnace.

Figure 14. Delayed Dose Decay for Mg_2SiO_4:Tb.

Each point is the average of three dosimeter readings. The error bars are the standard deviations. The line corresponds to a decay half life of 15 hr.

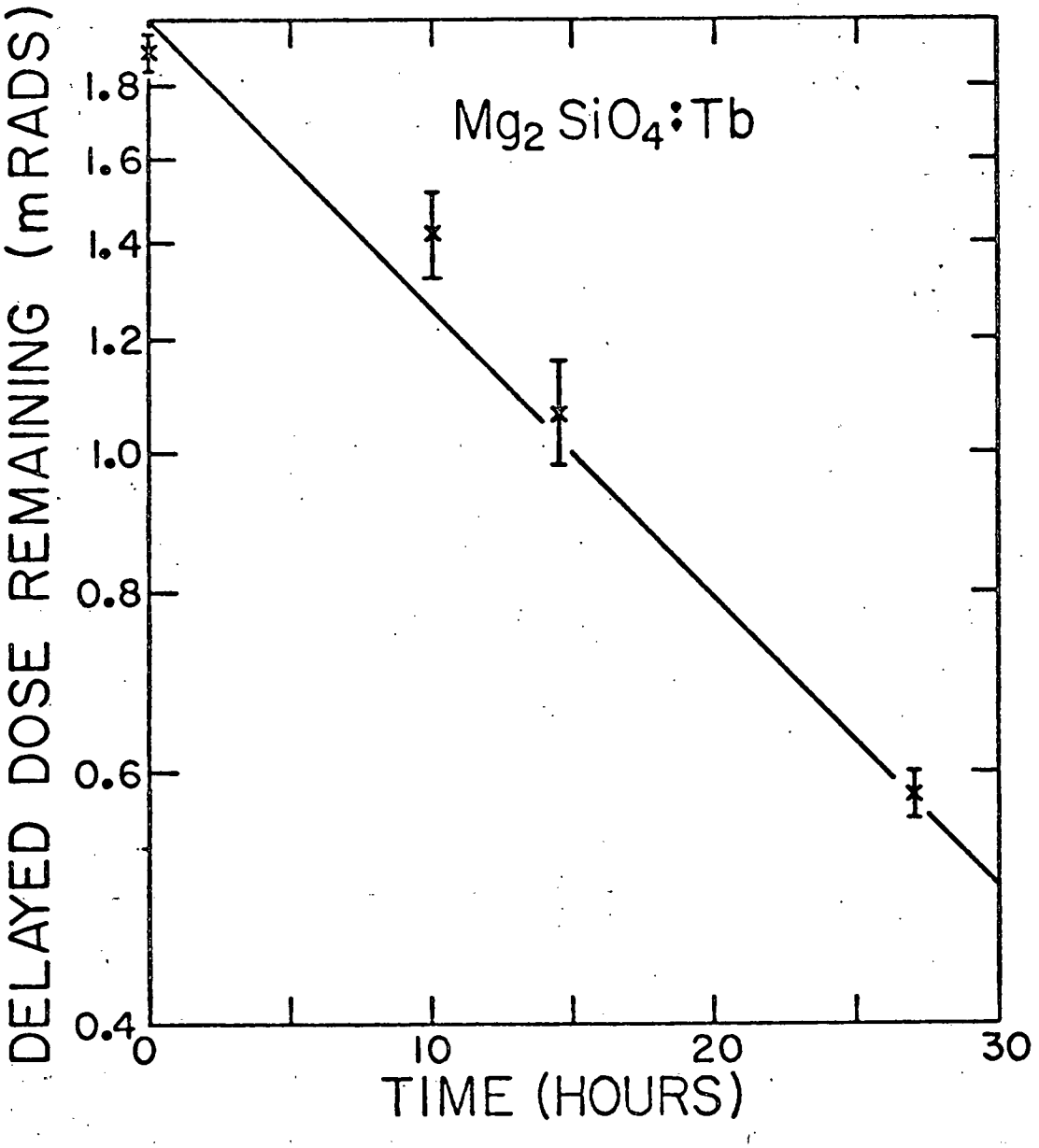
DELAYED DOSE REMAINING (mRADS)
1.8
1.6
1.4
1.2
1.0
0.8
0.6
0.4
0
10
20
30
TIME (HOURS)
Mg_2SiO_4:Tb

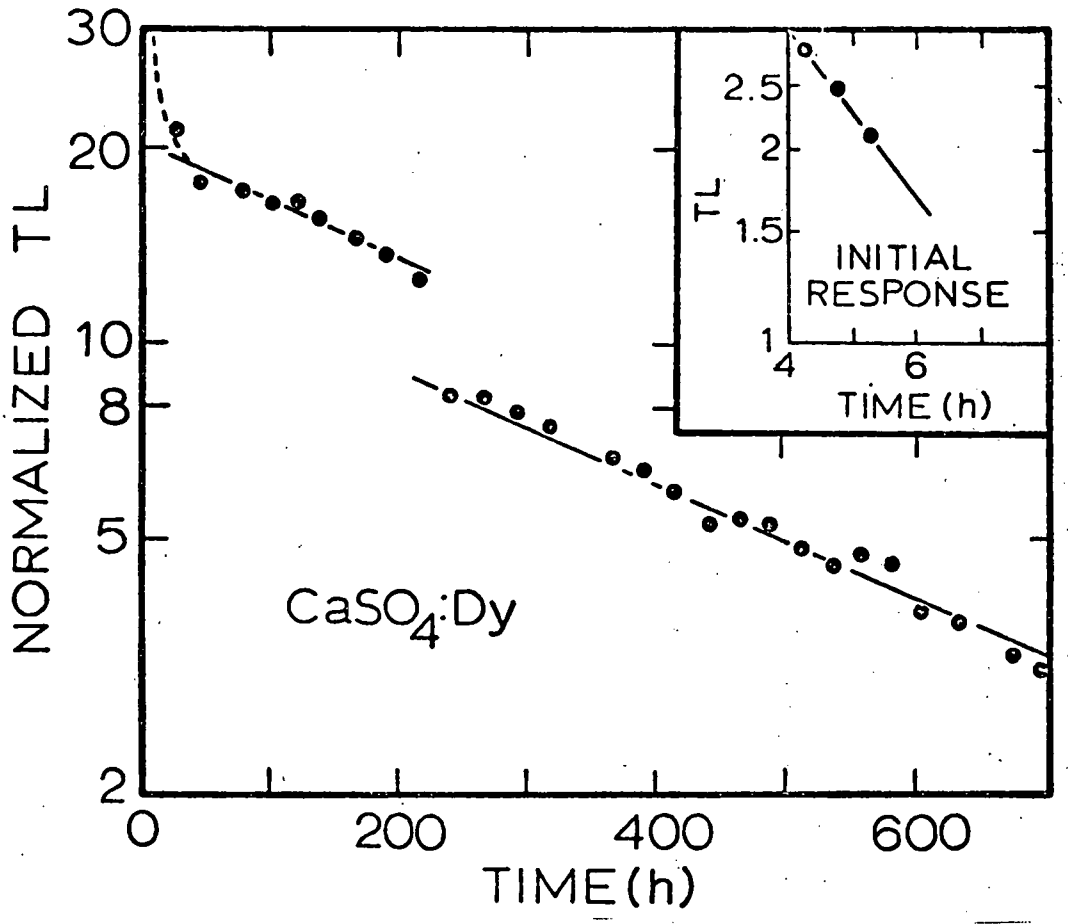

Figure 15. Delayed Dose Decay of $CaSO_4$:Dy.

The daily TL from self-irradiation as a function of time after irradiation in the reactor. The solid lines represent decay with the 343h half life of ^{32}P. The discontinuity results from annealing the sample 30 min at 600°C (see text). Since the self-irradiation times are not always identical, each TL reading is divided by $\exp(\Delta t/495)-1$. Insert: The initial TL due to 30 min self-irradiations. The solid line represents decay with the 2.32 h half life of ^{165}Dy. From Mayhugh and Watanabe.(1)

The net numbers of TL photons counted and the neutron fluences calculated from them using Eq. 18 and the measured sensitivities from Table V are given in Table VI. Corrections for the exposure time and the time delay to the end of the annealing were made.

The delayed dose in the CaF_2:Dy dosimeters is all from thermal neutron activation of the dysprosium since the fission averaged cross section for fluorine can be neglected. The one day delayed dose in the $CaSO_4$:Dy phosphor is also essentially all from the dysprosium activation. These two measurements indicated a rather uniform thermal neutron background of $1.5 \times 10^9 n/cm^2$ for a thirty minute exposure.

The 14 day delayed dose in the $CaSO_4$:Dy dosimeter is essentially all due to ^{32}P decay. Using the fission averaged cross section of 65mb, a fission spectrum fluence of $2.6 \pm 5 \times 10^{10} n/cm^2$ is calculated which is in good agreement with the $2.1 \times 10^{10} n/cm^2$ obtained with the conventional sulfur activation and ion chamber measurements. The fast neutron fluence in the penumbra was too small to measure by the delayed dose technique.

The delayed dose in the ZnO:Tm dosimeter comes both from thermal and fast neutrons. However, the $1.5 \times 10^9 n/cm^2$ thermal neutron fluence is so small that essentially all of the activation is due to fast neutrons. The fission spectrum fluence calculated is $2.6 \pm .2 \times 10^{10} n/cm^2$ taking the fission averaged cross section to be 35mb. The activation measured in the penumbra is of the correct order of magnitude but is comparable with the uncertainties in its measurement and the measurement of the background dose.

TABLE VI

Beam Port Activation Results

Phosphor	Location	Fluence	Energy	Cross Section
CaF_2:Dy	center	$1.57 \pm 0.02 \times 10^9 n/cm^2$	thermals	2.8 kb
	edge	$1.42 \pm 0.1 \times 10^9 n/cm^2$	thermals	2.8 kb
$CaSO_4$:Dy	center	$2.0 \pm 0.2 \times 10^9 n/cm^2$	thermals	2.8 kb
one day	edge	$2.4 \pm 0.5 \times 10^9 n/cm^2$	thermals	2.8 kb
$CaSO_4$:Dy	center	$2.6 \pm 0.5 \times 10^{10} n/cm^2$	fission	65 mb
	edge	$< 5 \times 10^9 n/cm^2$		
ZnO:Tm	center	$2.6 \pm 0.2 \times 10^{10} n/cm^2$	fission	35 mb
	edge	$< 2 \times 10^9 n/cm^2$		
Mg_2SiO_4:Tb	center	$1.6 \times 10^9 n/cm^2$ assumed	thermals	535 mb
		$2.1 \times 10^{10} n/cm^2$ assumed	fission	1.4 mb
		$3 \pm 1 \times 10^9 n/cm^2$ net	epithermal	600 mb
	edge	$1.5 \pm 0.8 \times 10^9 n/cm^2$	thermals	535 mb

In addition to the thermal and fast neutron sensitivities, the Mg_2SiO_4:Tb dosimeters respond to epithermal neutrons via resonances in the $^{23}Na(n,\gamma)^{24}Na$ reaction. The total resonance integral including the 1/v contribution is about 600mb, comparable with the thermal cross section of 535mb. The expected delayed dose from the thermal and fast neutron fluences can be calculated from Eq. 14 using the thermal cross section of 535mb and the fission cross section of 1.4mb. Ascribing the additional delayed dose which was observed to epithermal neutrons gives a fluence in the energy range to 3 keV of about $3 \times 10^9 n/cm^2$ for the thirty minute exposure.

14 MeV Neutron Attenuation: One of the possible applications of the delayed dose technique is measuring neutron fluence at various depths in a material where the small size and discrimination against gamma-rays are essential. The attenuation of 14 MeV neutrons by 2.7 cm of polyethylene was measured. The LiF:Mg,Ti dosimeters sensitized by the technique of Mayhugh and Fullerton[4] were used as these are the most sensitive dosimeters available which have only a fast neutron response. The high threshold energy of the fluorine activation discriminates against most of the scattered neutrons.

The geometry of the exposure is shown in Fig. 16. Three sensitized dosimeters were located at each of the points labeled A, B, and C. Three more from the same batch were retained for the background determination. A twenty minute neutron exposure gave a fluence of $1.1 \times 10^9 n/cm^2$ at the point A as measured by sulfur activation. All twelve dosimeters were annealed together for ten minutes at 300°C.

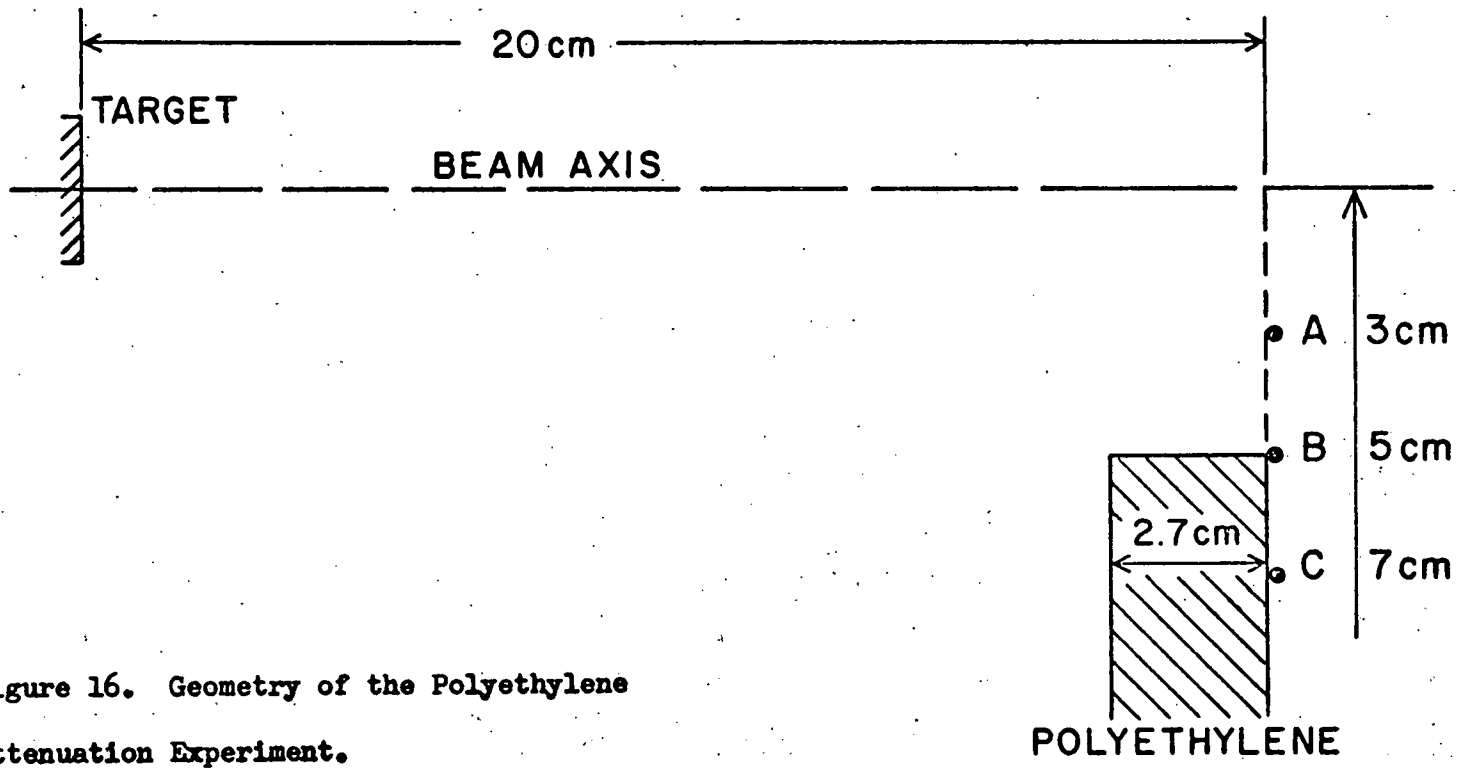

Figure 16. Geometry of the Polyethylene Attenuation Experiment.

This is the appropriate annealing to remove the prompt dose without affecting the sensitization. The correction for the irradiation time and the time interval to the end of the annealing amounted to 18%. The average photon counts corrected for background and decay are given in Table VII. The measured value for the attenuation is $.82 \pm .08$. Using a total cross section of 1.3 barns for CH_2 and a measured density of 0.95 gm/cm^3 for the polyethylene the calculated attenuation factor is $\exp(-l\sigma N/\rho) = 0.85$, where l is the path length, σ is the CH_2 total cross section, N is Avogadro's number and ρ is the density.

TABLE VII

Polyethylene Neutron Attenuation Results

Position	Average Counted Photons
A	8470 ± 87
B	8387 ± 100
C	6924 ± 542

REFERENCES

1. M. R. Mayhugh and Shigueo Watanabe, USAEC Report COO 1105-211, (1974).

2. L. Beach, E. Douple and D. W. Pearson, "Neutron and Gamma-ray Dosimetry at the Beam Port Irradiation Facility of the U.W. Nuclear Reactor." Unpublished Radio Therapy Center Report, March, 1973. U. W. Radio Therapy Center, Madison, Wis.

   J. R. Tesmer, D. W. Pearson and R. Moore, "Remeasurement of the Mixed Field Dose at Reactor Beam Port #4," unpublished, April, 1975. U. W. Physical Science Laboratory, Stoughton, Wis.

3. J. Moteff, "Radiation Dosimetry," Vol. III, Chpt. 21, P. 228, F. H. Attix and E. Tochlin, eds., Academic Press, New York, (1969).

4. M. R. Mayhugh and G. D. Fullerton, Health Physics 28, 297, (1975).

CHAPTER VII

DISCUSSION

This chapter discusses the results of this study of the delayed dose TL neutron activation dosimetry technique. The major advantage of passive solid state dosimeters over conventional activation detectors is given. The sensitivity of the delayed dose method is compared with conventional activation techniques. Limitations unique to the TL aspect of the technique are discussed. Each of the dosimeter phosphors studied is evaluated with respect to sensitivity, applicable neutron energy range and convenience of use. A discussion of the cross sections used is given. Three possible applications, radiation therapy dosimetry, personnel monitoring and fast neutron radiography are discussed.

Major Advantage: The major advantage of the delayed dose TL method over conventional activation detectors is that the actual recording of the neutron induced activity is accomplished without active electronics. The individual dosimeters themselves record a fraction of the total energy deposited by the radioactive decay in the form of the delayed dose TL signal. In terms of information this is a parallel process.

The actual readout of the delayed dose TL signal occurs after the activity has decayed and takes a time which is independent of the magnitude of the signal. The readout time is also very short compared to the half lives of the induced activities. The exact timing of the

TL readout is not critical on a time scale of hours, and serial reading of many dosimeters with a single instrument is appropriate. Thus the number of activation measurements which can be made from a single neutron exposure can be very large without requiring a vast array of counters. The processing of the dosimeters follows a program which is independent of the expected signal size and could be easily automated.

Sensitivity Considerations: It is interesting to compare the delayed dose neutron sensitivities with conventional neutron activation sensitivities. The number of activations produced in the dosimeters for a fluence of $10^7 n/cm^2$ at 14.7 MeV is given in Table VIII along with the number of TL photons which would be counted from the delayed dose. With the exception of the LiF and CaF_2:Mn dosimeters, the number of TL photons counted is greater than the number of activations induced. This comparison involves a TL reader whose overall detection efficiency is estimated to be around 1%. An improvement in this efficiency of a factor of ten could be obtained by a simple redesign of the optics of the reader. In any case it appears that the limitation on the neutron detection sensitivity by the delayed dose TL method is the number of activations produced in the dosimeters.

This comparison of the number of TL photons counted with the number of activations is an over-simplification. The delayed dose measures the energy deposited by the beta-rays not their number. Converting from the measured dose to a number, N, of beta decays involves assuming that each beta-ray deposited the average dose, or at least that

TABLE VIII

Relative Response for Fluence of $10^7 n/cm^2$, E_n = 14.7 MeV

Dosimeter	Isotope	Activations	TL Photons	Photons/ Activations
LiF:Mg,Ti	^{19}F	345	2.2	6.4×10^{-3}
CaF_2:Mn	^{19}F	500	250	0.5
CaF_2:Dy	^{19}F	270	740	2.7
Mg_2SiO_4:Tb	^{24}Mg	234	1260	5.4
ZnO:Tm *	^{64}Zn	7.4	28	3.6
$CaSO_4$:Dy *	^{32}S	9.3	336 **	36

---

* Per mg for a 100mg #5 gelatin capsule.

** For 14da, $t_{1/2}$, delay time.

$$N = \frac{1}{\bar{E}} \sum_{i=1}^{N} E_i \quad , \qquad 29$$

where $\bar{E}$ is the average beta energy deposited and the E_i are the actual energies deposited by each of the N betas. This is a good assumption for large N where it is essentially the definition of $\bar{E}$. However, the distribution in beta-ray energies introduces an uncertainty in addition to the number statistics of N, of an amount given by

$$\sigma_b^2 = N\left(\frac{\langle E^2 \rangle}{\langle E \rangle^2} - 1\right) \quad , \qquad 30$$

where $\langle E \rangle$ and $\langle E^2 \rangle$ are the first and second moments of the beta decay energy spectrum. (This is derived in Appendix II.) The smallest uncertainty possible for determining N decay betas from a dose measurement is then

$$\sigma^2 = N \frac{\langle E^2 \rangle}{\langle E \rangle^2} \quad . \qquad 31$$

The value of $\langle E^2 \rangle / \langle E \rangle^2$ depends on the details of the particular beta spectrum encountered but is in the range of 1 to 2. The precision obtainable with the delayed dose method should thus be within a factor of two of the ultimate limitation of the number statistics of N activations. This is approximately equivalent to a conventional activation detector system with the same number of atoms and a 25% efficient counter. (For $N > 10^3$, other error sources inherent in the TL dosimeters become dominant as is discussed later.)

It is important to point out that other fast neutron dosimetry techniques also have difficulty obtaining a large enough number of interactions to be significant. In particular, schemes to measure the proton recoil dose by embedding TL phosphor grains in an hydrogenous matrix or using proton radiator foil overlays on TL, TSEE (Thermally Stimulated Exoelectron) or TC (Thermocurrent) dosimeters will encounter the problem that the statistical fluctuations in the number of recoil protons will be a more important limit than the precision with which the proton dose received by a particular dosimeter can be measured.

For example, a $10^5 n/cm^2$ fluence of 14 MeV neutrons produces a total number of recoil protons of only 7×10^3 per gram of polyethylene. To get better than a 5% measurement, one must count at least ten per cent of these recoils. Because the recoil protons are distributed evenly in energy up to the maximum of 14 MeV, inferring the number of protons from a dose measurement increases the uncertainty another factor of about 9 from the ratio of $\langle E^2 \rangle / \langle E \rangle^2$ discussed previously. Again this is independent of the average amount of signal per proton recorded by the dosimeter. Measuring the entire recoil proton dose in one gram of polyethylene does not permit determination of the incident neutron fluence to better than about 5% when this fluence corresponds to a tissue dose of about 1 millirad.

Several characteristics which are unique to the TL dosimeters studied also affect the precision of the delayed dose measurement technique. Dosimeter reproducibility of better than 5% is difficult to achieve. This problem seems to be with the optical quality of

the dosimeters and with the reproducibility of their annealing, particularly their cooling rate. Variations in the optical quality of the dosimeter surfaces mean that the TL is emitted non-isotropically. Reproducibility therefore depends on accurate repositioning of the dosimeter during readout. A larger aperture light collection system, ideally 4π, in the reader would improve conditions somewhat and individual selection of the dosimeters can be helpful. Careful control of the annealing, particularly the cooling rate, has been shown to improve the reproducibility of LiF:Mg,Ti dosimeters.(1)

The fading of the TL in the CaF_2 based dosimeters also affects the reproducibility if a standard storage time is not used. In the measurements of the sensitivities given in the previous chapter, no correction for fading was made. The fading rate, ν, can be included explicitly. Using the terminology of Eq. 8,

$$\frac{1}{k}\frac{d}{dt}TL(t) = N_A(t_a)D_A f_A \lambda_A e^{-\lambda_A(t-t_a)} + d_B f_A - \nu TL(t). \qquad 32$$

The integrating factor is $\exp(\nu t_{ra})$ and the solution is

$$\frac{1}{k}TL(t_{ra}) = \frac{N_A(t_a)D_A f_A \lambda_A}{(\lambda_A - \nu)}\left(e^{-\nu t_{ra}} - e^{-\lambda t_{ra}}\right) + \frac{d_B f_B}{\nu}\left(1 - e^{-\nu t_{ra}}\right). \qquad 33$$

The effect of fading is to reduce the TL signal from CaF_2:Dy by less than 3% and from CaF_2:Mn by less than 5% per day.

The curious kinetics exhibited by Mg_2SiO_4:Tb are not easily treated rigorously. However, any error introduced must be no larger than about 30% of the dose received in the hour prior to the TL readout.

For a time interval, t_{ra}, of three days, this error is less than 1% of the total delayed dose TL signal. However, failure to wait for the TL signal to stabilize after a calibrating exposure could result in serious errors.

All TL dosimeters are polyatomic and contain various impurities including luminescent activators. In addition to the useful reactions listed in Table I, there are reactions with long lived products whose main effect is to increase the apparent background dose rate. The background dose which is subtracted to get the net delayed dose must include the contribution from the long lived radioactivity internal to the dosimeter. Thus the background dose rate appropriate to a dosimeter depends on its previous neutron exposure. As economics generally indicates reuse of the dosimeters, care must be taken to derive the correct background dose.

Since the number of activations per dosimeter is the main limitation to the sensitivity of the delayed dose method, only two approachs would seem to offer any promise for improvement. First the mass of the dosimeter could be increased. Bjarngard used 500mg samples of $CaSO_4$:Mn for microrad dosimeters.[2] That is more than ten times greater than the samples used in this study. Increasing the mass of the TL dosimeter would also increase the fraction of the decay energy absorbed if its geometry were not changed. Dosimeters perhaps ten times more massive than those presently used could be handled before the non-uniformity of their heating with the present system becomes a serious problem.

Secondly, one could look for activation reactions with larger cross sections. The present study was restricted to investigating currently available TL dosimeters. As these were developed for x-ray dosimetry with a tissue equivalent response desired, only relatively low atomic number materials have been studied. There are many optically transparent compounds of heavy elements with larger neutron cross sections which should be investigated. However the problem of finding a suitable fast neutron activation and a useful TL response in the same material is formidable.

Evaluation of Each Phosphor Type: From Fig. 12 one sees that none of the dosimeters studied is an ideal fast neutron detector. The fluorine reaction $^{19}F(n,2n)^{18}F$ is the best choice for measuring the primary beam fluence of 14 MeV neutrons. Because of the high threshold energy this reaction gives good discrimination against scattered neutrons. This discrimination allows the determination of the primary beam shape and penetration in a phantom although ignoring the scattered neutrons underestimates the dose at the measuring point. Only the LiF:Mg,Ti dosimeters do not have other, interfering reactions. Unfortunately, LiF is the least sensitive phosphor. However, dosimeters sensitized a factor of five by the technique of Mayhugh and Fullerton[3] show an adequate delayed dose TL for measurements of fluences appropriate to radiation therapy, e.g., $10^{10} n/cm^2$.

The CaF_2 based dosimeters have greater sensitivity than LiF although they contain fewer fluorines per gram. The CaF_2 phosphors are easily extruded or pressed into convenient forms. The main

problem with the dosimeters studied is that both activators, Dy and Mn, have large thermal neutron activation cross sections. Other activators with much smaller thermal cross sections would make excellent CaF_2 delayed dose activation detectors. CaF_2:Tm, for example, has recently become available in limited quantity,* and should be investigated.

The Mg_2SiO_4:Tb dosimeters have good fast neutron sensitivity over an energy range which covers the DT reaction, the Be(d,n) reaction and the higher energy neutrons from the fission spectrum, such as ^{252}Cf. The reasonably flat energy response gives a better measure of tissue dose in the presence of scattered neutrons than the fluorine reaction. The 15 hour half life of the product ^{24}Na is long enough not to limit the exposure times severely but does require a rather long wait for results. The thermal neutron sensitivity could be eliminated by encapsulation in some other glass such as fused quartz which has little activation.

The dosimeter with the broadest energy range is $CaSO_4$:Dy. The 14 day half life of the ^{32}P product, while advantageous for long exposure times requires an overly long wait for data. The thermal neutron response can be eliminated by using $CaSO_4$:Tm or simply separated from the fast neutron response by the two reading technique. The greatest problem with any $CaSO_4$ phosphor is that no solid forms are available. Powder dosimeters require too much extra handling to be convenient to use on a routine basis. Encapsulating the powder

---

* Harshaw Chemical Co., Solon, Ohio.

in fused quartz tubes would be one approach. Most other glasses have activation products which would interfere as noted in the case of the Mg_2SiO_4:Tb dosimeters. Embedding the phosphor in a polymer is unsuitable for two reasons. First, most polymers cannot tolerate high temperature annealing. Second, all of the polymer embedded phosphors tested exhibit residual or spurious light signals of the order of tens of millirads which make the measurement of the small TL signal from the delayed dose impossible.

The value of the ZnO:Tm dosimeter is difficult to assess. The phosphor has adequate fast neutron sensitivity with a broad energy dependence, and very low thermal neutron sensitivity. The samples used were all powders and little is known about the possibility of making solid dosimeters from this material. Considerably better characterization of this phosphor is needed.

Cross Sections: Some comments on cross sections are in order. Most cross sections are not well known. A brief look at a compilation of cross sections such as BNL 325[4] which displays the experimental data collected shows that disagreements of factors of 2 or 3 are not rare. Such discrepancies are of course outside the error limits claimed. There is also a serious lack of data in the difficult energy range between 8 and 12 MeV. In many cases the choice of cross section is rather arbitrary. The variation of the cross section with neutron energy is usually more consistent and can be calculated reasonably well. For this reason the sensitivity functions plotted in Fig. 12 are believed to be of some value although it would be interesting to check them at another neutron energy.

The cross sections actually used in calculations are given either in the text or in the appropriate tables. The fluorine cross section was taken from tabulated values in the UK Neutron Data Library.[5] The sulfur activation cross section was taken from Allen, et al.[6] The magnesium cross section was from BNL 325 Supplement 2.[4] The zinc cross section curve was taken from a calculation by Ringle[7] normalized to measurements in BNL 325. The dysprosium cross section was taken from BNL 325.

The values of the fission averaged cross section which is defined by

$$\bar{\sigma}_{fission} \equiv \frac{\int_0^{E_{max}} \sigma(E)\, \phi_{fission}(E)\, dE}{\int_0^{E_{max}} \phi_{fission}(E)\, dE} \qquad 34$$

come from a variety of sources. For the sulfur reaction, $\bar{\sigma}_f$=65mb is a reasonably agreed upon value given by Moteff.[8] Santry and Butler[9] suggest 63.6 mb and Depuydt and Mevergnies[10] report measuring 65±3mb. The value 35 mb was chosen for the zinc reaction. Boldeman[11] measured 27 mb which is quoted by Moteff,[8] but Santry and Butler[9] measured 34 mb and Kimura, et al[12] report 35 to 37 mb. The fission averaged cross section for the magnesium reaction was taken as 1.4 mb which is the value measured by Kimura, et al.[12] Santry and Butler[9] calculated 1.38 mb and Bresesti, et al[13] measured 1.26 mb.

Possible Applications: Three areas of potential application were considered: Fast neutron radiation therapy, personnel monitoring and neutron radiography. For fast neutron radiation therapy, the

neutron fluences are likely to be high, (of the order of 10^{10} n/cm^2, 100 rads = 1.5×10^{10} n/cm^2) and delivered in a few minutes. Current practice for many tumors is to deliver the dose in 100 - 200 rad fractions on alternate days to a total dose of a few thousand rads. The dose fractions must be delivered in times short enough to expect a patient not to move.

For 14 MeV neutrons from the D-T reaction, all of the dosimeters considered have adequate sensitivity for measurements out to the 5% dose contours - 10^9 n/cm^2. The body is a large moderator and scattered neutrons down to thermal energies are present. The high threshold energy of the fluorine reaction gives the best discrimination against these scattered neutrons. Only the LiF dosimeter has no appreciable activations beside the fluorine reaction. The two hour half life of the fluorine nuclide ensures that the dosimetry results would be available the following day in time to make alterations to the next treatment if needed.

Activation detectors are not particularly attractive as personnel fast neutron monitors. Personnel dosimetry requires a detector response which is proportional to integral dose over a long time at very low doses. Radionuclides with half lives long enough to have an activity proportional to fluence over a long monitoring period have induced activities too small to be measured easily. In addition, the energy dependence of the activation cross section does not usually correspond to the biological response as expressed by the neutron quality factor. However, for short monitoring times or as personnel accident dosimeters, activation detectors have some potential.

Of the reactions studied, only the sulfur activation is of any real interest. Its cross section is reasonably flat with energy from 3 to 15 MeV. The half life of ^{32}P of 14 days allows a working week--5 days--to be monitored with a worst case loss of activity of only 22% if all the neutron exposure were received on the first day. The delayed dose integrating time of two weeks is not unreasonable for low exposures and could be shortened if a large exposure were received as from an accident. The problem of adequate sensitivity remains. Personnel exposures of the order of millirads, $10^5 n/cm^2$, must be measurable. From Table VIII one sees that this fluence corresponds to about one activation per 3 mg of $CaSO_4$, and that some method of increasing the activity is required.

The conventional sulfur activation technique burns the sulfur to concentrate the ^{32}P from a large sulfur mass. By including a small amount, 100 to 200 mg, of $CaSO_4$:Dy in a 100 gm sulfur pellet when burned, the ^{32}P can be concentrated on the $CaSO_4$ grains. The delayed dose measurement of this ^{32}P activity proceeds as described in Chapter III. Although no detailed investigation of the quantitative yields has been made, preliminary experiments show about half of the ^{32}P activity in the sulfur pellet was deposited on the $CaSO_4$ grains when burned. Replicate measurements using the same sulfur mass, the same phosphor mass and the same size and shape burning pan agreed to about 3%, better than the normal errors in reading the $CaSO_4$:Dy TL. Both the TL and the residual activity in the burning pan were measured. Using this technique sulfur pellets of 100 gm would give adequate sensitivity for measuring fluences of the order of $10^5 n/cm^2$ equivalent to about one millirad.

A major difficulty with fast neutron radiography is the lack of suitable detectors. Radiographic film is very insensitive to fast neutrons while being quite sensitive to thermal neutrons and gamma-rays. Even using plastic scintillator screens in front of the film, the ratio of fast neutron to gamma-ray sensitivity is only about 0.1 on a rad for rad basis.[14] A thermal neutron fluence of 10^{10} n/cm^2 gives about the same developed film density as one rad of gamma-rays. The possibility of eliminating gamma-ray and thermal neutron interference by using the sulfur threshold reaction and a film to record the activation, the activation transfer method, was investigated by Tochlin.[14] The fast neutron doses required to produce an image were too high, 10^4 rads, to be of any biological or medical interest.

With the delayed dose method, point by point reconstructions of fast neutron images are possible at fluences of 10^9 n/cm^2, corresponding to about a 10 rad tissue dose. From Table VII, the results of the attenuation experiment of Fig. 16, the present resolution would correspond to about a centimeter of polyethylene. In the plane of the detector, the spatial resolution would be determined by the size and shape of the dosimeters but could not be smaller than the range of the decay beta-rays, a few tenths of a millimeter. For an incident beam of 14 MeV neutrons and the fluorine threshold reaction, neutrons scattered by protons through more than 10° are effectively removed. The removal cross section is thus a combination of the absorption and scattering cross sections. The scattered neutrons do not contribute any diffuse background signal to the image.

REFERENCES

1. G. D. Fullerton, private communication, July, 1975.
2. B. E. Bjarngard, Report AE-118, Aktiebolaget Atomenergi, Stockholm, Sweden, (1963).
3. M. R. Mayhugh and G. D. Fullerton, Health Phys. 28, 297, (1975).
4. BNL 325, Supplement 2, Superintendent of Documents, U. S. Government Printing Office, Washington, D. C. 20402.
5. United Kingdom Neutron Data Library, NDL 1972, UKAEA, Harwell, U. K.
6. L. Allen, Jr., W. A. Biggers, R. J. Prestwood and R. K. Smith, Phys. Rev. 107, 1363, (1957).
7. J. Ringle, UCRL 10732, U. of Cal. Rad. Lab, Berkeley, CA, (1963).
8. J. Moteff, Chpt. 21, Vol. III, in Radiation Dosimetry, F.H.Attix and E. Tochlin, eds., Academic Press, New York, (1969).
9. D. C. Santry and J. P. Butler, AECL 3521, Atomic Energy of Canada Limited, Chalk River, Ontario, Canada.
10. H. Depuydt and M. N. Mevergnies, J. Nucl. Energy A/B, 16, 447, (1962).
11. J. W. Boldeman, J. Nucl. Energy 18, 417, (1964).
12. I. Kimura, K. Kobayashi and T. Shibata, J. Nucl. Sci. and Tech. 8, 59, (1971).
13. A. M. Bresesti, M. Bresesti and R. A. Rydin, Nucl. Sci. Eng. 29, 7, (1967).
14. E. Tochlin, Phys. Med. Biol. 10, 477, (1965).

APPENDIX I

OPTIMAL DELAYED DOSE READOUT TIME

The choice of delayed dose readout time involves consideration of both experimental convenience and maximum TL signal. The latter depends on the amount of activation, the background radiation level in the storage area and the dark count rate of the reader. For a given measurement the number of TL photons ascribed to the delayed dose signal, N_s, is given by

$$N_S = (N - N_d) - (N_b - N_d) \pm \sqrt{fN^2 + fN_b^2 + fN_d^2}\,, \qquad \text{AI1}$$

where N is the number of photons counted from the first heating, N_d is the dark count which is subtracted during the reheat, and N_b is the number of photons counted from the background radiation. The fluctuations in the signal, background and dark count are represented by fN, fN_b and fN_d respectively. The fluctuations in the dark counts do not follow a poisson distribution due to multiple correlated pulses, but the fluctuations in the signal and background do. The ratio of net signal to error is then

$$S/E = N_s / \sqrt{N + N_b + fN_d^2}\,. \qquad \text{AI2}$$

From Eq. 7 we have

$$N_S = N_{S\,max}(1 - \exp -\lambda t_{ra})\,, \qquad \text{AI3}$$

and

$$N_b = d_B f_B t_{ra} \quad , \qquad \text{AI4}$$

apart from a factor giving the particular reader sensitivity. Taking $k = \lambda t_{ra}$, $b = d_B f_B$, and $d = f N_d^2$ and setting the derivative with respect to k equal to zero, we have

$$N_{s\,max}\, e^{-k}(1-e^{-k}) + \frac{b}{\lambda}(2ke^{-k} + e^{-k} - 1) + de^{-k} = 0 . \qquad \text{AI5}$$

This derivative was evaluated for values of N_{smax} from 100 to 10^5 and the values of λ, b and d characteristic of each of the different dosimeter types. The ranges of the solutions of Eq. AI5 are given in Table A I.

TABLE A I

Dosimeter	Decay Constant λ	Storage Time for Maximum TL
LiF:Mg,Ti	0.38/hr	$5/\lambda$ to $7/\lambda$; 13 to 18 hours
CaF_2:Dy	0.38/hr	$4/\lambda$ to $6/\lambda$; 10 to 16 hours
CaF_2:Mn	0.38/hr	$4/\lambda$ to $6/\lambda$; 10 to 16 hours
Mg_2SiO_4:Tb	0.0465/hr	$2/\lambda$ to $4/\lambda$; 43 to 86 hours
ZnO:Tm	0.0465/hr	$4/\lambda$ to $6/\lambda$; 86 to 120 hours
$CaSO_4$:Dy	0.002/hr	$1/\lambda$ to $3/\lambda$; 21 to 60 days

APPENDIX II

The incident neutron fluence is related to the number, N, of activations produced. When the dose from the decay of these N activations is measured, the relation $D=N\bar{d}$ must be used to calculate N, where $\bar{d}$ is the average dose per decay. ($\bar{d}$ is the same as D_A of Eq. 9.) For large N this relation is essentially a definition of $\bar{d}$. However, for small N it is important to know the additional uncertainty introduced by assuming that each decay deposits the average dose.

The probability that the dose D came from N decays of average dose $\bar{d}$ is

$$P(D)=\int\cdots\int\prod_{j=1}^{N}p(d_j)\,dd_j\,\delta\left(N\bar{d}-\sum_{k=1}^{N}d_k\right)\ , \qquad \text{AII1}$$

where $p(d_j)$ is the probability that the j^{th} decay deposits a dose d_j and the delta function insures that the total dose is D. The rms fluctuation in the number N is given by $\sigma_N^2=\langle N^2\rangle-\langle N\rangle^2$. The expectation values $\langle N^2\rangle$ and $\langle N\rangle$ are given by

$$\langle N\rangle=\int\cdots\int_{}^{N+1}\prod_{j=1}^{N}p(d_j)\,dd_j\,N\,\delta\left(N\bar{d}-\sum_{k=1}^{N}d_k\right)\ , \qquad \text{AII2}$$

and

$$\langle N^2\rangle=\int\cdots\int_{}^{N+1}\prod_{j=1}^{N}p(d_j)\,dd_j\,N^2\,\delta\left(N\bar{d}-\sum_{k=1}^{N}d_k\right). \qquad \text{AII3}$$

Integrating over N in Eq. AII2 gives

$$\langle N\rangle = \int_{\cdots}^{N}\int \prod_{j=1}^{N} p(d_j)\,dd_j \,\frac{1}{\bar{d}}\sum_{k=1}^{N} d_k \quad . \qquad \text{AII4}$$

The remaining N integrals give $\bar{d}$ each time j=k, so that

$$\langle N\rangle = \frac{N\bar{d}}{\bar{d}} = N \quad . \qquad \text{AII5}$$

Eq. AII3 can be integrated over N to give

$$\langle N^2\rangle = \int_{\cdots}^{N}\int \prod_{j=1}^{N} p(d_j)\,dd_j \,\frac{1}{\bar{d}^2}\sum_{k=1}^{N} d_k \sum_{l=1}^{N} d_l \quad . \qquad \text{AII6}$$

The remaining N integrals can be broken down as

$$\langle N^2\rangle = \frac{1}{\bar{d}^2}\int_{\cdots}^{N}\int \left\{\sum_{k\neq l}^{N} d_k \sum_{l=1}^{N} d_l \prod_{j=1}^{N} p(d_j) + \sum_{l=1}^{N} d_l^2 \prod_{j=1}^{N} p(d_j)\right\} dd_j \quad . \qquad \text{AII7}$$

Then

$$\langle N^2\rangle = \frac{1}{\bar{d}^2}\left[(N-1)N\langle d\rangle^2 + N\langle d^2\rangle\right] \quad . \qquad \text{AII8}$$

Remembering that $\bar{d} = \langle d\rangle$ gives

$$\langle N^2\rangle = \left(N^2 - N + \frac{N\langle d^2\rangle}{\langle d\rangle^2}\right) \quad . \qquad \text{AII9}$$

Then

$$\sigma_N^2 = N^2 - N + \frac{N\langle d^2\rangle}{\langle d\rangle^2} - N^2 \quad . \qquad \text{AII10}$$

$$\langle N\rangle = \int\cdots\int^{N} \prod_{j=1}^{N} p(d_j)\,dd_j \,\frac{1}{\bar{d}} \sum_{k=1}^{N} d_k \quad . \qquad \text{AII4}$$

The remaining N integrals give $\bar{d}$ each time j=k, so that

$$\langle N\rangle = \frac{N\bar{d}}{\bar{d}} = N \quad . \qquad \text{AII5}$$

Eq. AII3 can be integrated over N to give

$$\langle N^2\rangle = \int\cdots\int^{N} \prod_{j=1}^{N} p(d_j)\,dd_j \,\frac{1}{\bar{d}^2} \sum_{k=1}^{N} d_k \sum_{l=1}^{N} d_l \quad . \qquad \text{AII6}$$

The remaining N integrals can be broken down as

$$\langle N^2\rangle = \frac{1}{\bar{d}^2}\int\cdots\int^{N} \left\{ \sum_{k\neq l}^{N} d_k \sum_{l=1}^{N} d_l \prod_{j=1}^{N} p(d_j) + \sum_{l=1}^{N} d_l^2 \prod_{j=1}^{N} p(d_j) \right\} dd_j \quad . \qquad \text{AII7}$$

Then

$$\langle N^2\rangle = \frac{1}{\bar{d}^2}\left[(N-1)N\langle d\rangle^2 + N\langle d^2\rangle\right] \quad . \qquad \text{AII8}$$

Remembering that $\bar{d} = \langle d\rangle$ gives

$$\langle N^2\rangle = \left(N^2 - N + \frac{N\langle d^2\rangle}{\langle d\rangle^2}\right) \quad . \qquad \text{AII9}$$

Then

$$\sigma_N^2 = N^2 - N + \frac{N\langle d^2\rangle}{\langle d\rangle^2} - N^2 \quad . \qquad \text{AII10}$$

Finally,

$$\sigma_N^2 = N\left(\frac{\langle d^2\rangle}{\langle d\rangle^2} - 1\right) . \qquad \text{AII11}$$